Escola de Camins
Escola Tècnica Superior d'Enginyeria de Camins, Canals i Ports
UPC BARCELONATECH

TREBALL FINAL DE GRAU

Computational modelling of fracture: gradient damage models with variable internal length

Treball realitzat per:

Guillermo Segura Valdivieso

Dirigit per:

Antonio Rodríguez-Ferran

Grau en:

Enginyeria Civil

Barcelona, juny de 2017

Departament d'Enginyeria Civil i Ambiental

ABSTRACT

Computational modelling of fracture: gradient damage models with variable internal length

Fracture modelling has always been a direction of research in engineering, more specifically in civil engineering. In this last quarter of century, the implementation of nonlocality in damage models has been a direction of study for materials fracture, more specifically for quasi-brittle materials such as concrete or rocks. This type of damage model allows a more accurately characterization of the behavior of this type of materials and it has been seen that it is not possible to accurately model the behavior of this materials without a nonlocal formulation, because it characterizes the behavior of the material as a whole, weighting the value of a variable of a point on its neighborhood.

This dissertation aims for an investigation on new models able to characterize the damage effect on quasi-brittle materials. In this direction, this thesis focuses on models with a variable internal length which sees its value reduced due to the increase on damage. Furthermore, two models in this dissertation are presented on how to treat this internal length reduction.

One model presents an unbounded internal length reduction allowing a vanish of its value for high damage values, whereas the other model do not allow a null value of the internal length, even for high damage values, imposing a minimum value –threshold– for the internal length.

Finally, both models and an original model with a constant internal length –where these two models are based from– are tested on a uniaxial strain and stress problem and its results and parameters discussed.

TABLE OF CONTENTS

First chapter

1 INTRODUCTION

1.1 MOTIVATION

Determining the behaviour of materials under loads is not only important in civil engineering, but also in fields like aeronautic or industrial engineering. Consequently, modelling the response of a material under a wide different boundary conditions is necessary for the day-to-day.

This dissertation focusses on modelling the response of quasi-brittle materials, such as concrete or ceramic materials under uniaxial stress and strain conditions. For those types of materials its inelastic deformation is characterized by micro cracks and micro voids, that progressively deteriorate the stiffness of the affected zone. The general approach to compute this kind of behaviour is to use a nonlocal formulation in order to model the continuum behaviour of the sample. This nonlocal formulation can be implemented with

a.) Integral-type nonlocal model.
b.) Nonlocal gradient models. Including explicit and implicit models.

Exploring new applications of these models and new nonlocal gradient models is the aim of this dissertation. Because when fracture development is controlled and its behaviour modelled, we could start talking about fracture success and not about fracture failure. As in reinforcement concrete, where the fracture of the concrete is totally controlled and the structural element is designed for it, if we could control the fracture development in other material and for other applications we could expand this idea of fracture success to other fields.

1.2 NONLOCAL MODELS

Despite mechanical behaviour of solids has been assumed to be only local dependant in the past, ergo the deformation is characterized only by the deformation gradient and the deformation history, it has become clear that damage in material cannot be adequately characterized by local constitutive relation between stress and strain tensors thought the past quarter of a century. The reason behind it is that the stress at a point should depend on the hold body. And not only stresses, also strains at a point depend on the hold body, see Bažant et al. (2001).

1.2.1 Integral-type models

This type of models solves the nonlocal effect by defining the constitutive law at a point weighting averages of the state of a variable on the neighbourhood of that point, see Bažant et al. (2001). That can be formulated taking $Y(x)$ as the local variable defined in a domain V so the corresponding nonlocal variable is defined as

$$\tilde{Y}(x) = \int_V \alpha(x,\xi) Y(\xi) d\xi \tag{1.1}$$

such that α is the nonlocal weighting function that is often taken as the Gauss distribution function

$$\alpha(x,z) = \exp\left(-\frac{n_{dim} r^2}{2l^2}\right) \tag{1.2}$$

where l is called the **internal length** and n_{dim} is the number of dimensions (1, 2 or 3). In order to clarify the nonlocal effect, a 2D example in formulation can be useful, defining $Y(x)$ as the local variable in a domain V_x

$$\tilde{Y}(x) = \int_{V_x} \alpha(x,z) Y(z) dz \tag{1.3}$$

such that

$$\alpha(x,z) = \exp\left[-\left(\frac{\|x-z\|}{l}\right)^2\right] \tag{1.4}$$

Integral-type models are easier to understand compared to nonlocal gradient models, where the interaction between is the local and nonlocal variable is defined as an implicit equation. But, nowadays for characterizing the behaviour of brittle materials affected by damage is usually done with nonlocal gradient models.

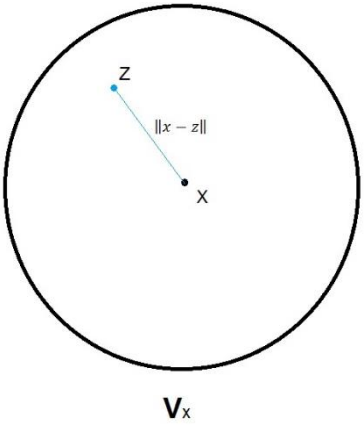

Figure 1: Sketch of the neighbourhood effect in 2D.

1.2.2 Nonlocal gradient models

Gradient models can be divided in two categories of gradient models: Explicit gradient models and implicit gradient models. As in the models explained in the following chapters are nonlocal implicit gradient models only this type of models is explained in this dissertation. For more information about explicit gradient model formulation can be found in Bažant et al. (2001).

The nonlocal implicit formulation defines $\tilde{Y}$ as the solution of a diffusion-reaction PDE

$$\tilde{Y} - l^2 \nabla^2 \tilde{Y} = Y \; in \; \Omega \tag{1.5}$$

with homogeneous Newmann boundary conditions

$$\nabla \tilde{Y} \cdot \boldsymbol{n} = 0 \; on \; \partial\Omega \tag{1.6}$$

the new model is based on the implicit formulation but wants to explore the implications of having a non-constant internal length, which sees its value reduced in the areas where the damage appears. In fact, this internal length reduction reduces the damage distribution capability of the material in areas where the damage appears, as it is proved in this dissertation.

Moreover, a new internal length parameter is defined

$$c = l^2 \tag{1.7}$$

1.3 DAMAGE EFFECT

As it has been already explained, nonlocal models are a good approach for describing the damage effect in some materials. This effect can be considered in the constitutive equation as

$$\sigma = (1 - d(\varepsilon))E\varepsilon \tag{1.8}$$

where, d is the damage parameter defined as a variable that can go from 0 (no damage) to 1 (zero cohesion between elements). The damage effect it is considered to be a linear, so the stiffness is reduced when damage increase, that is totally reasonable since having less cohesion leads to a reduction of the Young modulus. The damage parameter has been defined as

$$d(\varepsilon) = \frac{\varepsilon_u(\varepsilon - \varepsilon_i)}{\varepsilon(\varepsilon_u - \varepsilon_i)} \tag{1.9}$$

where ε_i is the lower bound threshold where the damage starts and ε_u is the maximum strain that an infinitesimal element can support. So, the final constitutive equation responds to a **linear softening** behaviour

$$\sigma = E\frac{\varepsilon_i(\varepsilon_u - \varepsilon)}{\varepsilon_u - \varepsilon_i} \tag{1.10}$$

in spite of having an **internal length** variable as a new way of study, this study is not aiming for a new damage effect on the constitutive equation and will remain untouched.

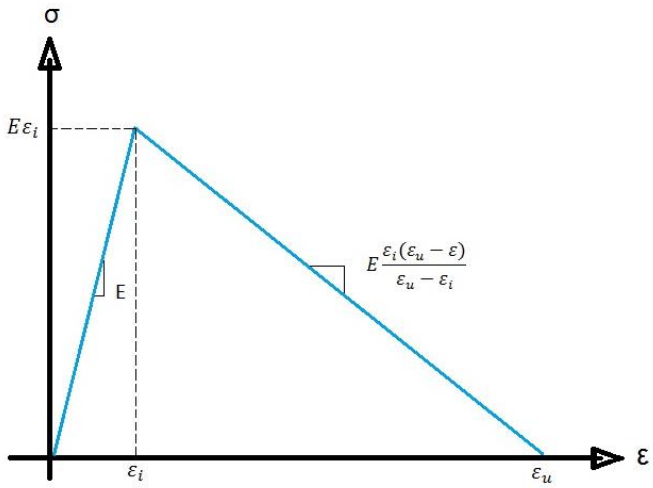

Figure 2: Constitutive relation with linear softening.

Second chapter

2 ORIGINAL MODEL

2.1 MODEL WITH CONSTANT INTERNAL LENGTH

The original model from which the new model is based on was presented in Rodríguez-Ferran et al. (2005). In this chapter, this model is also introduced and explained in order to compare it to the new model.

As it has been explained thought this document there are different types of nonlocal models, this one is an implicit gradient damage model that can be used in a one-dimension problem, for instance a uniaxial test.

In the original model the second-order PDE relates the nonlocal displacement $\tilde{\boldsymbol{u}}$ with the local displacement $\boldsymbol{u}$. Consequently, the boundary conditions for the diffusion-reaction PDE were adapted passing from Newmann to Dirichlet conditions. The reason on doing that is further explained in the original paper but these conditions allows to be reproducible in order one, also have a clear physical interpretation: local and nonlocal displacement must coincide in all the boundary domain. From the following strong form

$$\tilde{u} - c\nabla^2\tilde{u} = u \; on \; \Omega \tag{2.1}$$

$$\tilde{u}(x) = u(x) \; on \; \partial\Omega \tag{2.2}$$

where c is the new notation for the **square of the internal length**, the weak form obtained using a FEM discretization, see Original model in Annex A: Weak form discretization, remains as

$$[\boldsymbol{M} + c\boldsymbol{D}]\tilde{\boldsymbol{u}} = \boldsymbol{M}\boldsymbol{u} \tag{2.3}$$

which is the **regularization equation**. Furthermore, the damage parameter is the one shown in equation 1.9 which now depends on the nonlocal deformation which produces **linear softening** in the constitute equation.

Table 1: Original model one dimension problem.

Stress-strain relation	$\sigma = (1 - d(\tilde{\varepsilon}))E\varepsilon$	(2.4)
Local strains	$\varepsilon(x) = \dfrac{du(x)}{dx}$	(2.5)
Nonlocal displacements	$\tilde{u}(x) - c\dfrac{d}{dx}\left[\dfrac{d\tilde{u}(x)}{dx}\right] = u(x)$ $\tilde{u}(x) = u(x) \quad on\ \partial\Omega$	(2.6)
Nonlocal strains	$\tilde{\varepsilon}(x) = \dfrac{d\tilde{u}(x)}{dx}$	(2.7)
Damage evolution	$d(\tilde{\varepsilon}) = \dfrac{\varepsilon_u(\tilde{\varepsilon} - \varepsilon_i)}{\tilde{\varepsilon}(\varepsilon_u - \varepsilon_i)}$	(2.8)

2.2 UNIAXIAL TENSILE TEST

This model was verified in uniaxial tension test. Imposing some weakened elements (10% reduction in the Young's modulus) in the central part of a beam and applying no load steps but displacement steps.

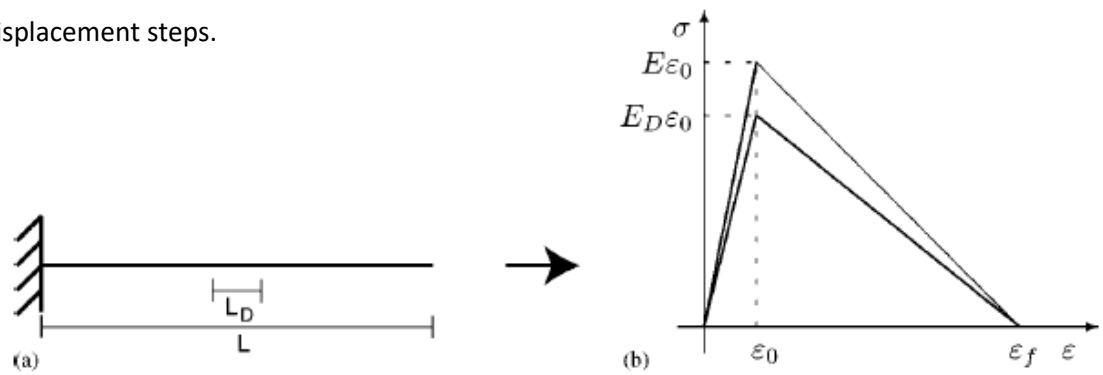

Figure 3: Uniaxial tension test: (a) problem statement; and (b) linear softening law.

Table 2:Uniaxial tension test. Geometric and material parameters.

Meaning	Symbol	Value	Units
Length of bar	L	100	mm
Idem of weaker part	L_D	10	mm
Cross-section of bar	A	1	mm
Young's modulus	E	20000	MPa
Idem of weaker part	E_D	18000	MPa
Damage threshold	ε_i	10^{-4}	
Final strain	ε_f	$1.25 \cdot 10^{-4}$	
Prescribed displacement	u_{pr}	0.0001	mm

In order to solve this problem, two related equations must be solved at the same time: the **equilibrium equation** and the **regularization equation**, that can be formulated as

$$Equilibium\ equation\colon\ \boldsymbol{f_{int}}(\boldsymbol{u},\tilde{\boldsymbol{u}}) = \boldsymbol{f_{ext}} \tag{2.9}$$

$$Regularization\ equation\colon\ [\boldsymbol{M} + c\boldsymbol{D}]\tilde{\boldsymbol{u}} = \boldsymbol{M}\boldsymbol{u} \tag{2.10}$$

obviously as mentioned before there are no external forces applied but displacements are imposed at the end of the beam in each step, so the external forces are always null. Then the left part of the equation, that is local and nonlocal displacement dependant must be zero in each step the boundary conditions are

$$\begin{cases} u_0 = \tilde{u}_0 = 0 \\ u_f = \tilde{u}_f = u_{pr} \end{cases} \tag{2.11}$$

it has to be mentioned that imposing boundary conditions always carry out reaction forces and this problem is not an exception, this consideration is explained deeply in the section 2.3 Solving the uniaxial tensile problem.

2.2.1 Results obtained

Once the model is discussed and the problem to be solved explained, it can be presented the typical results that can be obtained with this model. Some of the figures presented below were already calculated and shown in the original paper of the model, but it has been recalculated aiming for a deeper knowledge of how the original model works.

All the presented figures below have been obtained using a *c* value of 5 and 320 elements.

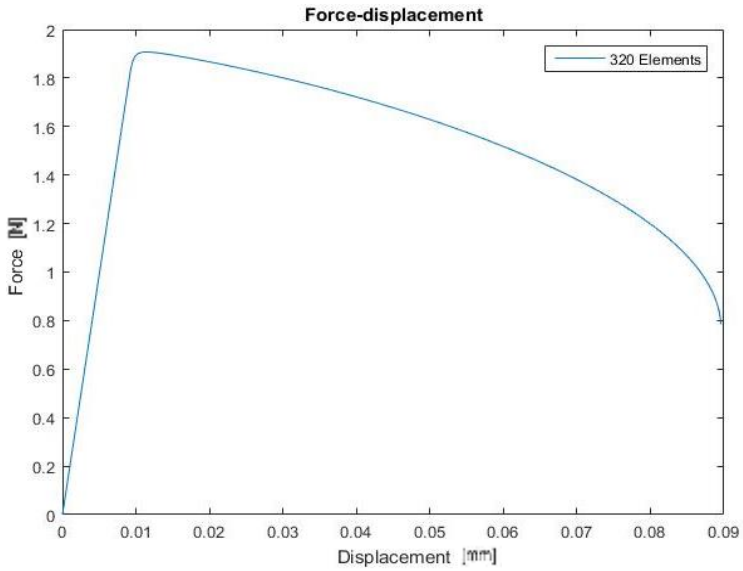

Figure 4: Force-displacement relation in the original model.

Figure 4 displays the force-displacement relation which due to the effect of damage in the constitutive equation 2.4 once the deformation reaches the lower bound threshold ε_i the linear softening starts to take place and the force-displacement relation passes from a linear behaviour ruled by the Young's modulus value to the nonlinear behaviour ruled by the damage and the Young's modulus. This plot stops when one element of the mesh reaches the damage value of 1, that means zero cohesion between elements (fracture).

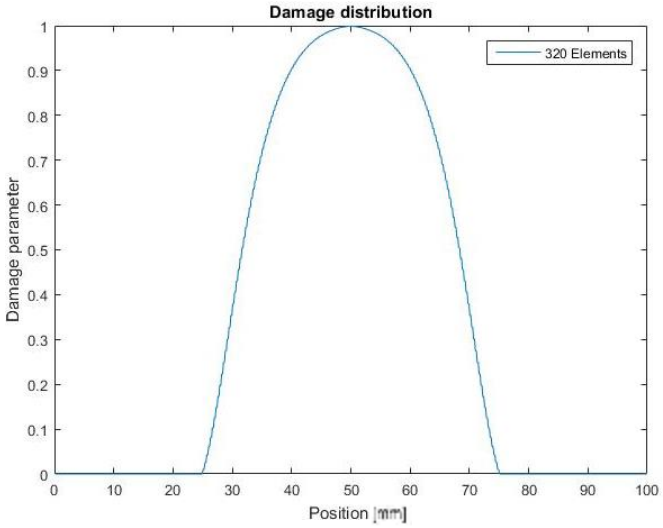

Figure 5: Damage distribution in the original model.

Figure 5 shows the typical response of the damage distribution in the last step using this model. As it can be seen it concentrates in the weakened central elements but is still spread outside the weakened zone (10%). It goes without saying that having a weakened zone on a beam confers it less resistance but with this model where the damage has a very impactful appearance the consequence of having a weakened zone is even worse because as it can be seen in *figure 5*, for this case with a *c* value of 5, the beam breaks when there are still plenty of elements undamaged.

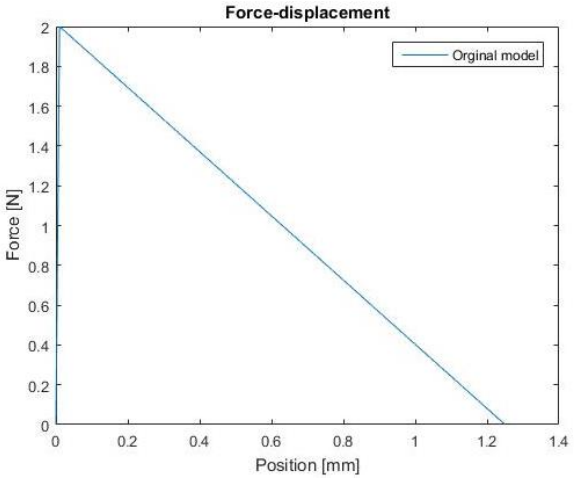

Figure 6: Force-displacement without any weakened elements using the original model.

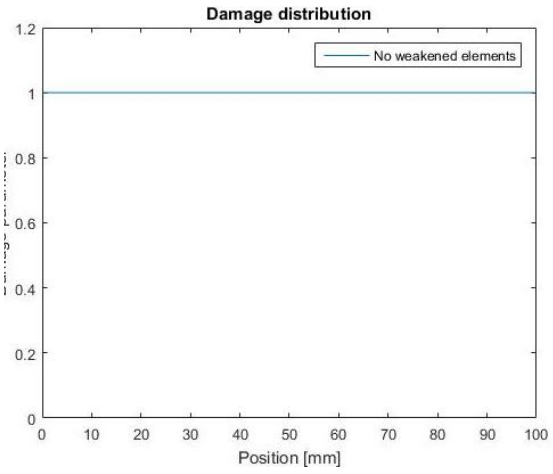

Figure 7: Damage distribution without any weakened elements using the original model.

Whereas if the beam does not have any weakened elements -*figure 6* and *figure 7*- a homogeneous distribution of the damage is obtained and perfect linear softening behaviour is obtained, which is a far more ductile behaviour than the one described by *figure 4*.

2.3 SOLVING THE UNIAXIAL TENSILE PROBLEM FOR THE MODEL WITH CONSTANT INTERNAL LENGTH

This model was coded in MATLAB and it is based in the FEMLAB code for FEM, see Hededal et al. (1995). As presented before, in each displacement step, which does the function of a time step, two equations must be solved

$$Equilibrium\ equation: \quad \boldsymbol{f_{int}}(\boldsymbol{u}, \tilde{\boldsymbol{u}}) + \boldsymbol{f_{reac_{equi}}} = \boldsymbol{f_{ext}} \tag{2.12}$$

$$Regularization\ equaton: \quad [\boldsymbol{M} + c\boldsymbol{D}]\tilde{\boldsymbol{u}} + \boldsymbol{f_{reac_{regu}}} = \boldsymbol{Mu} \tag{2.13}$$

now the reaction forces are clearly separated from the rest of the terms, in the paper presented in 2005 those reactions were treated using the **penalty method** but looking forwards to the new model, the calculation of reactions has been implemented using **Lagrange multipliers**, see Annex B: Lagrange multipliers, that allow linear boundary conditions which are applied in the regularization equation and indeed this regularization equation is affected in the new model for having a variable internal length.

The internal forces can be calculated using the Gauss-Legendre quadrature for integrations

$$\boldsymbol{f_{int}}(\boldsymbol{u}, \tilde{\boldsymbol{u}}) = \sum_{p} w_p \sigma_p(\boldsymbol{u}, \tilde{\boldsymbol{u}}) \tag{2.14}$$

and the discretization of the strong form leads to a mass and diffusivity matrix as

$$\boldsymbol{M} = \int_{\Omega} N^T N \, dV \quad and \quad \boldsymbol{D} = \int_{\Omega} \nabla N^T \nabla N \, dV \tag{2.15}$$

one way of solving this problem is imposing that the error of the regularization equation 2.13 and the error of the equilibrium equation 2.12 must be null in each step

$$\boldsymbol{r_{equi}} := -\boldsymbol{f_{ext}} + \boldsymbol{f_{int}}(\boldsymbol{u}, \tilde{\boldsymbol{u}}) + \boldsymbol{f_{reac_{equi}}} = \boldsymbol{0} \tag{2.16}$$

$$\boldsymbol{r_{regu}} := -\boldsymbol{Mu} + [\boldsymbol{M} + c\boldsymbol{D}]\tilde{\boldsymbol{u}} + \boldsymbol{f_{reac_{regu}}} = \boldsymbol{0} \tag{2.17}$$

to solve this root finding problem in each iteration the **Newton method** for nonlinear problems was chosen. Newton method is characterized for approximating the next step value using a Taylor expansion of first order as

$$f({}^{n+1}x) \approx f({}^{n}x) + \Delta({}^{n+1}x) \cdot \frac{df}{dx}({}^{n}x) \tag{2.18}$$

to obtain a more accurate result each step is iterated the needed amount of times, so equation 2.18 is modified and remains as

$$f({}^{n+1}x) \approx f({}^{n}x) + \Delta({}^{n+1}x^{i}) \cdot \frac{df}{dx}({}^{n}x^{i}) \tag{2.19}$$

Even this model that has multiple variables to be calculated in each step can be simplified as the following problem

$$\boldsymbol{K}(\boldsymbol{x})\Delta\boldsymbol{x} = \boldsymbol{f} \tag{2.20}$$

and

$$\boldsymbol{K}(\boldsymbol{x})\boldsymbol{\delta x} = \boldsymbol{f} \tag{2.21}$$

where $\boldsymbol{K}(\boldsymbol{x})$ is the always called stiffness matrix and $\Delta\boldsymbol{x}$ or $\delta\boldsymbol{x}$ is the vector formed by all the unknown variables that want to be calculated. The stiffness matrix is dependent on the variables that forms vector $\Delta\boldsymbol{x}$ or $\delta\boldsymbol{x}$. In this problem, these variables are the nonlocal displacements $\tilde{\boldsymbol{u}}$, the local displacements $\boldsymbol{u}$ and the reaction forces of the equilibrium and regularization equation due to the boundary conditions. $\boldsymbol{f}$ is the vector formed by the residual of the equilibrium equation and the residual of the regularization equation, which in this model is always null because it is a linear equation and the Taylor expansion for this equation is not an approximation but an exact solution. At the first iteration in each new step the nonlinear system to solve is

$$\begin{pmatrix} {}^{k}\boldsymbol{K}_{\boldsymbol{uu}} & {}^{k}\boldsymbol{K}_{\boldsymbol{u\tilde{u}}} & \boldsymbol{A}^{T} & 0 \\ \boldsymbol{K}_{\tilde{\boldsymbol{u}}\boldsymbol{u}} & \boldsymbol{K}_{\tilde{\boldsymbol{u}}\tilde{\boldsymbol{u}}} & 0 & \boldsymbol{A}^{T} \\ \boldsymbol{A} & 0 & 0 & 0 \\ 0 & \boldsymbol{A} & 0 & 0 \end{pmatrix} \begin{pmatrix} {}^{k+1}\Delta\boldsymbol{u} \\ {}^{k+1}\Delta\tilde{\boldsymbol{u}} \\ {}^{k+1}\Delta\boldsymbol{\lambda}_{\boldsymbol{equi}} \\ {}^{k+1}\Delta\boldsymbol{\lambda}_{\boldsymbol{regu}} \end{pmatrix} = \begin{pmatrix} -{}^{k}\boldsymbol{r}_{\boldsymbol{equi}} \\ 0 \\ \boldsymbol{B} \\ \boldsymbol{B} \end{pmatrix} \tag{2.22}$$

where $\boldsymbol{B}$ and $\boldsymbol{A}$ are the used constant matrixes for implementing the boundary conditions via the Lagrange multipliers method and $\boldsymbol{\lambda_{equi}}$ and $\boldsymbol{\lambda_{regu}}$ are the Lagrange multipliers, calculated in order to compute the reaction forces.

Obviously, in the first iteration the gradients of the local and nonlocal displacements and the gradient of the Lagrange multipliers are calculated due to imposing the prescribed displacement u_{pr} via boundary conditions. For further iterations in the same step only the error is corrected so the problem to solve can be expressed as

$$\begin{pmatrix} {}^{k}\boldsymbol{K}_{uu}{}^{i} & {}^{k}\boldsymbol{K}_{u\tilde{u}}{}^{i} & \boldsymbol{A}^{T} & 0 \\ \boldsymbol{K}_{\tilde{u}u} & \boldsymbol{K}_{\tilde{u}\tilde{u}} & 0 & \boldsymbol{A}^{T} \\ \boldsymbol{A} & 0 & 0 & 0 \\ 0 & \boldsymbol{A} & 0 & 0 \end{pmatrix} \begin{pmatrix} {}^{k+1}\boldsymbol{du}^{i+1} \\ {}^{k+1}\boldsymbol{d\tilde{u}}^{i+1} \\ {}^{k+1}\boldsymbol{d\lambda_{equi}}{}^{i+1} \\ {}^{k+1}\boldsymbol{d\lambda_{regu}}{}^{i+1} \end{pmatrix} = \begin{pmatrix} {}^{k}-\boldsymbol{r_{equi}}{}^{i} \\ 0 \\ 0 \\ 0 \end{pmatrix} \tag{2.23}$$

where

$$\boldsymbol{K}_{uu} = \frac{\partial r_{equi}}{\partial u} = \sum_{p} w_p (1 - d_p) E \tag{2.24}$$

$$\boldsymbol{K}_{u\tilde{u}} = \frac{\partial r_{equi}}{\partial \tilde{u}} = \sum_{p} w_p E \varepsilon_p \, d'_p \tag{2.25}$$

$$\boldsymbol{K}_{\tilde{u}u} = \frac{\partial r_{regu}}{\partial u} = \boldsymbol{M} \tag{2.26}$$

$$\boldsymbol{K}_{\tilde{u}\tilde{u}} = \frac{\partial r_{regu}}{\partial \tilde{u}} = \boldsymbol{M} + c\boldsymbol{D} \tag{2.27}$$

$${}^{k+1}\boldsymbol{u} = {}^{k}\boldsymbol{u} + {}^{k+1}\Delta\boldsymbol{u} + {}^{k+1}\boldsymbol{du}^{i} \tag{2.28}$$

$${}^{k+1}\tilde{\boldsymbol{u}} = {}^{k}\tilde{\boldsymbol{u}} + {}^{k+1}\Delta\tilde{\boldsymbol{u}} + {}^{k+1}\boldsymbol{d\tilde{u}}^{i} \tag{2.29}$$

$${}^{k+1}\boldsymbol{\lambda_{equi}} = {}^{k}\boldsymbol{\lambda_{equi}} + {}^{k+1}\Delta\boldsymbol{\lambda_{equi}} + {}^{k+1}\mathbf{d}\boldsymbol{\lambda_{equi}}{}^{i} \tag{2.30}$$

$${}^{k+1}\boldsymbol{\lambda_{regu}} = {}^{k}\boldsymbol{\lambda_{regu}} + {}^{k+1}\Delta\boldsymbol{\lambda_{regu}} + {}^{k+1}\boldsymbol{d\lambda_{regu}}{}^{i} \tag{2.31}$$

$\boldsymbol{K}_{uu}$ and $\boldsymbol{K}_{u\tilde{u}}$ are the called secant and the local tangent matrices respectively and as it can be seen in equation 2.23 and equation 2.24 are calculated via integrals using a Gauss-Legendre quadrature in each iteration, whereas the tangent and secant matrices are constant through all the problem because the regularization equation is linear in this model.

To consider that the approximation of each iteration is good enough different conditions has been used to control it: (a) the relative error in displacement and (b) the relative error in forces must be less than an imposed threshold (tol). Which can be formulated as

$$(a)\ tol_u > \frac{\left\| {}^{k+1}\boldsymbol{du}^i \right\|}{\left\| {}^{k}\boldsymbol{u} + {}^{k+1}\Delta\boldsymbol{u} \right\|} \tag{2.32}$$

$$(b)\ tol_{equi} > \frac{\left\| \boldsymbol{r_{equi}} \right\|}{\left\| \boldsymbol{f_{reac_{equi}}} \right\|} \tag{2.33}$$

Third chapter

3 NEW MODELS WITH VARIABLE INTERNAL LENGTH

3.1 PRESENTING THE MODELS

The new models are a modified version of the original model presented above which tries to explore the implications of having a **variable internal length**. Having a variable internal length tries to model a structural behaviour of damage concentration in the already damaged zones. In order to model this behaviour, reducing the internal length as the damage increases, that it is the variable that softens the damage and distribute it over the whole body of the sample, it is a proper idea for a first approach.

In this direction, two methods have been explored:

a.) **Unbounded diffusion reduction**: the reduction on the internal length due to damage is not limited and can reach zero.

b.) **Bounded diffusion reduction**: a chosen threshold is imposed in the diffusion-reaction PDE so the diffusion parameter, that makes the problem a nonlocal problem, never reaches a null value.

The main difference between these models is that in non-limited diffusion reduction model when the damage gets high values the problem becomes a local model, whereas in model with a limited diffusion reduction this never happens due to the imposed threshold.

3.1.1 New model with variable internal length and unbounded diffusion reduction

Having a variable internal length and non-limited reduction of it can be formulated in the diffusion-reaction PDE as

$$\tilde{u} - \frac{d}{dx}\left[c[1 - d(\tilde{u})]\frac{d\tilde{u}}{dx}\right] = u \tag{3.1}$$

$$\tilde{u} = u \qquad on\ \partial\Omega \tag{3.2}$$

the same boundary conditions are used in this model as in the original and the weak form obtained is

$$[\boldsymbol{M} + c\boldsymbol{D}(\tilde{\boldsymbol{u}})]\tilde{\boldsymbol{u}} = \boldsymbol{M}\boldsymbol{u} \tag{3.3}$$

this weak form is the new regularization equation, see Annex A: Weak form discretization, and as it can be seen is not linear anymore, since the diffusion matrix is nonlocal displacements dependant.

Table 3: New model with variable internal length and unbounded diffusion reduction applied in one dimension.

Stress-strain relation	$\sigma = (1 - d(\varepsilon))E\varepsilon$	(3.4)
Local strains	$\varepsilon(x) = \frac{du(x)}{dx}$	(3.5)
	$\tilde{u}(x) - \frac{d}{dx}\left[c[1 - d(\tilde{u}(x))]\frac{d\tilde{u}(x)}{dx}\right] = u(x)$	(3.6)
Nonlocal displacements	$\tilde{u} = u \qquad on\ \partial\Omega$	(3.7)
Nonlocal strains	$\tilde{\varepsilon}(x) = \frac{d\tilde{u}(x)}{dx}$	(3.8)
Damage evolution	$d(\tilde{\varepsilon}) = \frac{\varepsilon_u(\tilde{\varepsilon} - \varepsilon_i)}{\tilde{\varepsilon}(\varepsilon_u - \varepsilon_i)}$	(3.9)

As in the original model the equilibrium equation and the new regularization equation must be solved in each step. Having a nonlinear regularization equation affects different equations to solve the problem, but this is further explained in section 3.3 Solving the .

3.1.2 New model with variable internal length and bounded diffusion reduction

The only difference between this model and the model with a vanishing internal length is in the reduction parameter, a new parameter called a has been introduced in the diffusion-reaction PDE so the reduction due to damage never reaches zero

$$\tilde{u} - \frac{d}{dx}\left[c[1 - ad(\tilde{u})]\frac{d\tilde{u}}{dx}\right] = u \quad on\ \Omega \tag{3.10}$$

$$\tilde{u} = u \quad on\ \partial\Omega \tag{3.11}$$

where a has always a value smaller than 1, allowing a lower bound threshold in the reduction parameter

$$[1 - ad(\tilde{u})] \tag{3.12}$$

even when damage increases to one, due to the effect of a this reduction parameter is never zero. Preventing a null value of the internal length means always having a nonlocal problem even for high damage values. As the other variables have remained untouched the weak form obtained using a FEM discretization is similar to the one obtained with a non-limited diffusion reduction

$$[\boldsymbol{M} + c\boldsymbol{D}(\tilde{\boldsymbol{u}})]\tilde{\boldsymbol{u}} = \boldsymbol{M}\boldsymbol{u} \tag{3.13}$$

but now the diffusion matrix $\boldsymbol{D}(\tilde{\boldsymbol{u}})$ includes the parameter a.

Table 4: New model with variable internal length and bounded diffusion reduction applied in one dimension.

Stress-strain relation	$\sigma = (1 - d(\varepsilon))E\varepsilon$	(3.14)
Local strains	$\varepsilon(x) = \frac{du(x)}{dx}$	(3.15)
	$\tilde{u}(x) - \frac{d}{dx}\left[c[1 - ad(\tilde{u}(x))]\frac{d\tilde{u}(x)}{dx}\right] = u(x)$	(3.16)
Nonlocal displacements	$\tilde{u} = u \quad on\ \partial\Omega$	(3.17)
Nonlocal strains	$\tilde{\varepsilon}(x) = \frac{d\tilde{u}(x)}{dx}$	(3.18)
Damage evolution	$d(\varepsilon) = \frac{\varepsilon_u(\varepsilon - \varepsilon_i)}{\varepsilon(\varepsilon_u - \varepsilon_i)}$	(3.19)

3.2 UNIAXIAL TENSILE TEST

In order to compare these new models with the original one, both models have been tested under the same problem that the original model was tested. As mentioned before is a uniaxial stresses and strains problem with a weakened zone in the central part of the beam

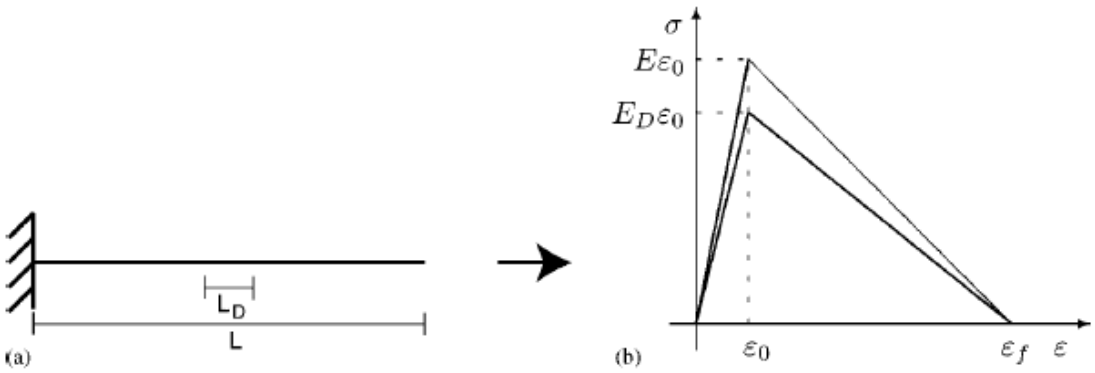

Figure 8: Sketch of the problem under which the new models are tested.

Table 5: Values of the problem.

Meaning	Symbol	Value	Units
Length of bar	L	100	mm
Idem of weaker part	L_D	10	mm
Cross-section of bar	A	1	mm
Young's modulus	E	20000	MPa
Idem of weaker part	E_D	18000	MPa
Damage threshold	ε_i	10^{-4}	
Final strain	ε_f	$1.25 \cdot 10^{-4}$	
Prescribed displacement	u_{pr}	0.0001	mm

As in the original problem, in order to solve the problem two related equations must be solved at the same time

$$Equilibium\ equation: \quad \boldsymbol{f_{int}}(\boldsymbol{u}, \tilde{\boldsymbol{u}}) = \boldsymbol{f_{int}} \tag{3.20}$$

$$Regularization\ equation: \quad [\boldsymbol{M} + c\boldsymbol{D}(\tilde{\boldsymbol{u}})]\tilde{\boldsymbol{u}} = \boldsymbol{M}\boldsymbol{u} \tag{3.21}$$

but now the regularization equation is not linear anymore because the diffusion matrix depends on damage, that at the same time is a variable dependant on the nonlocal displacements $\boldsymbol{D}(\tilde{\boldsymbol{u}})$. The imposed displacements applied via boundary conditions are

$$\begin{cases} u_0 = \tilde{u}_0 = 0 \\ u_f = \tilde{u}_f = u_{pr} \end{cases} \tag{3.22}$$

as mentioned before imposing boundary conditions always carry out reaction forces and this problem is not an exception. This consideration is explained deeply in the section 3.3 Solving the

.

3.2.1 Results obtained.

Even though the models seem pretty similar when are presented, the same problem calculated with the two different models leads to substantially different behaviours. Both models are presented in the same plots so a quick comparison between them can be done. A more deeply comparison of all three models is presented in chapter 4.

All the charts shown below have been calculated with 320 elements and with the original parameters of the problem.

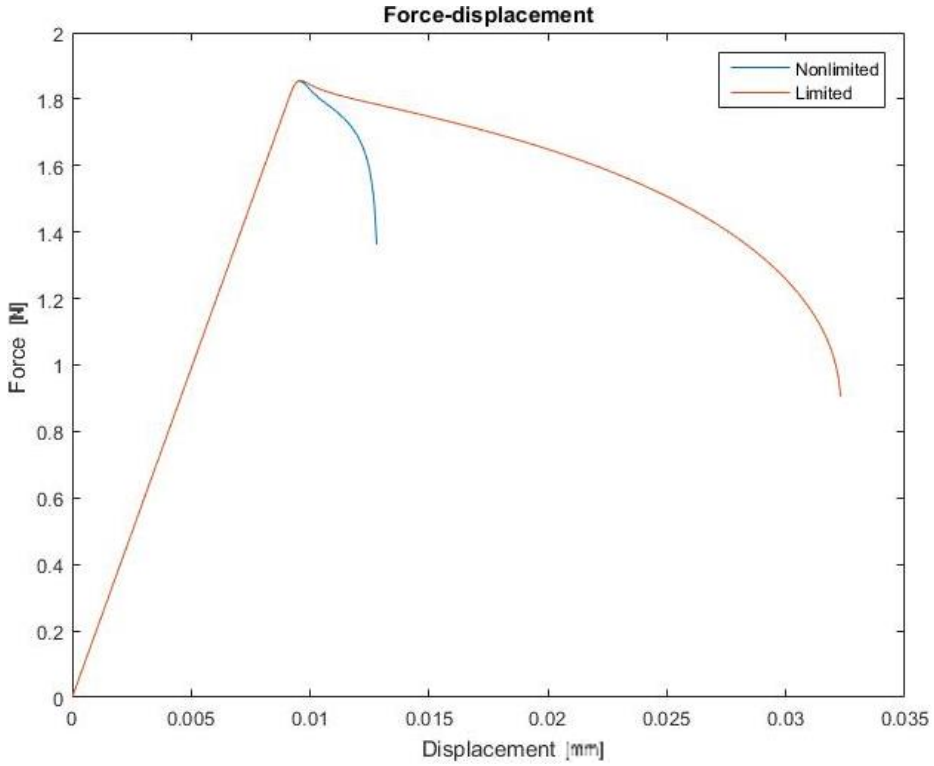

Figure 9: Force-displacement chart of both models with a variable internal length.

As it can be seen *figure 9* shows how the model with a limited internal length reduction exhibits a more ductile behaviour than the other model. What is totally expected from the models presented, where the more ductile one has a minimum internal length value, which allows a more distributed damage along the beam as can be seen in *figure 10*.

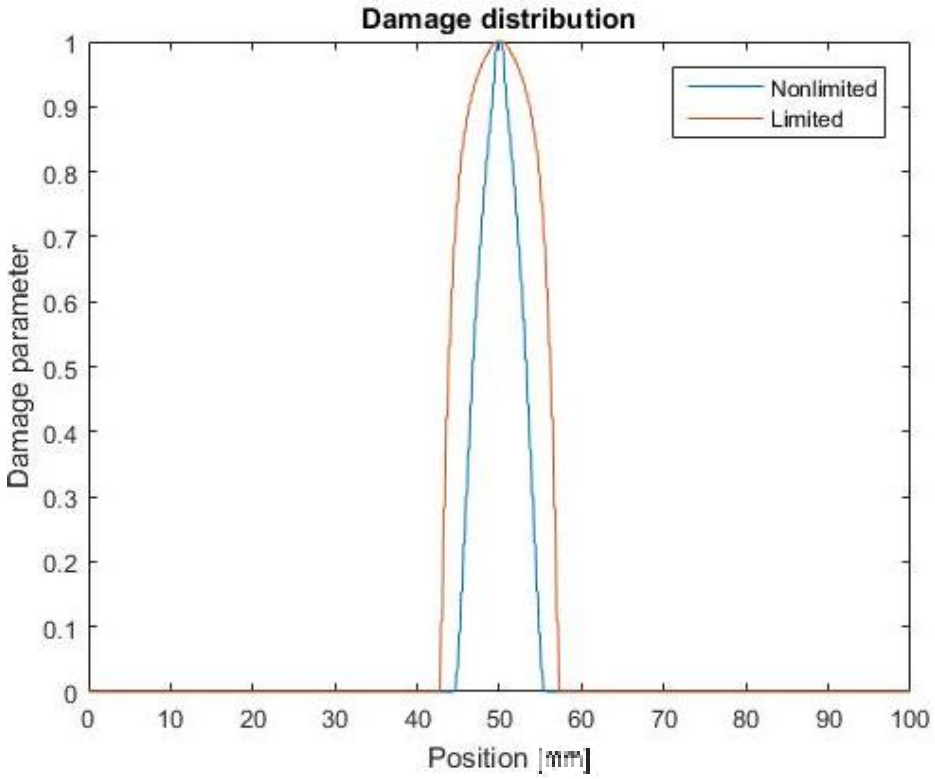

Figure 10: Damage distribution in the last step of the uniaxial problem for both models with a variable internal length.

Comparing both models' last step damage distribution, it can be said that in both models the damage is concentrated in the central element but in the model with an unbounded reduction of the internal length shows a steeper slope of the damage parameter in figure 10. Whereas the model with a lower bound threshold value of the internal length shows damaged element with a higher damage parameter meaning that the damage is able to distribute along more elements before reaching the value of one in the central element.

Furthermore, in *figure 11* the a parameter shows that does not only affect the last displacement steps, as it could be thought, but it has an effect at the early nonlinear steps, when the damage starts. Having the a parameter multiplying the effect of damage on the internal length means a

higher c values from the first nonlinear steps in the bounded internal length reduction model. Leading to a wider distribution of damage since the beginning of the damage appearance.

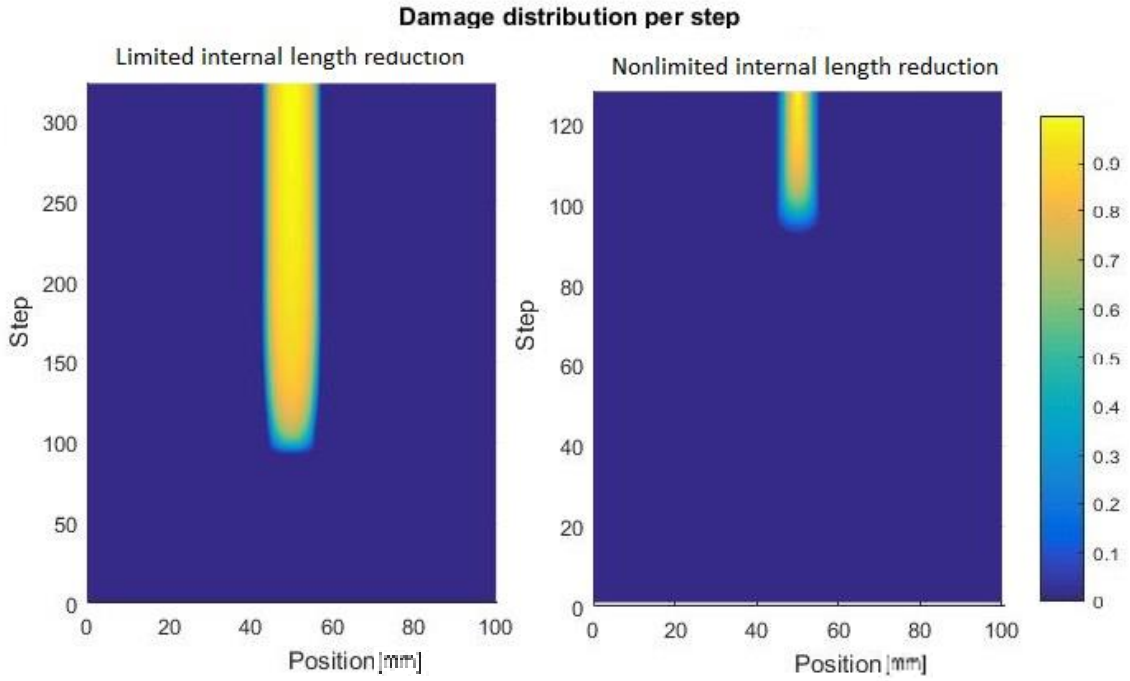

Figure 11: Damage distribution per step comparison between the new models.

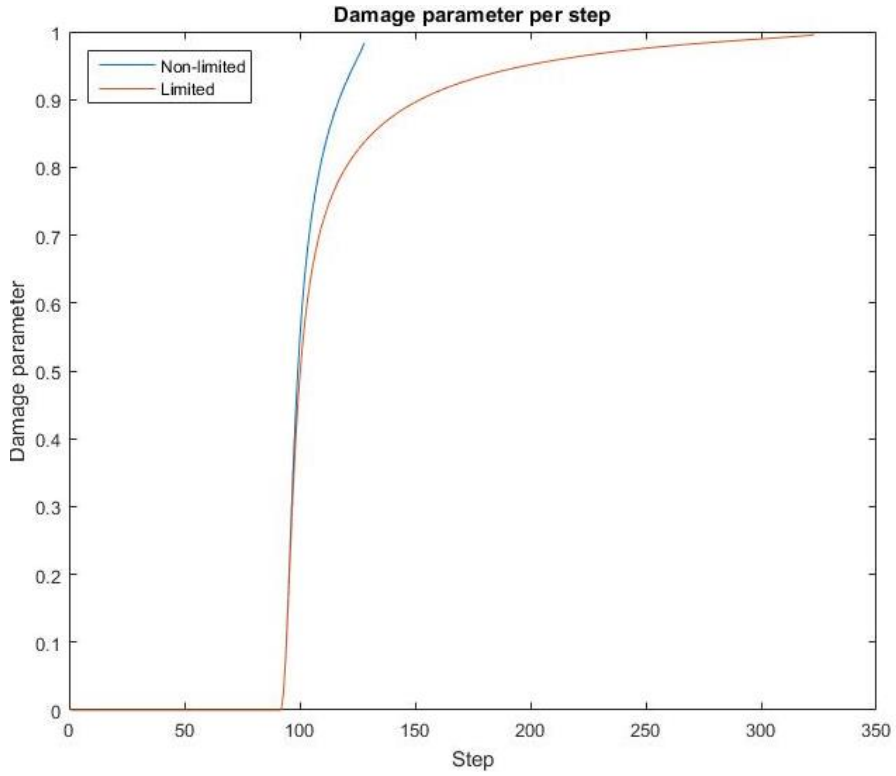

Figure 12: Central element damage parameter development through the steps for the two models.

Figure 12 shows the influence of the parameter a as a threshold in the damage effect over the internal length. The model with a bounded internal length reduction describes a curve with a softener damage slope when the damage gets higher allowing the beam to resist more displacement steps. Whereas the other curve, without this threshold, the damage slope does not suffer this smoothing and the central element reaches the fracture in less steps.

3.3 SOLVING THE UNIAXIAL TENSILE PROBLEM FOR THE MODEL WITH VARIABLE INTERNAL LENGTH

As for the original model this model has been implemented in MATLAB. In order to do that, all the code wrote has been based on the initial model, using Lagrange multipliers for the boundary conditions, and in the FEMLAB code.

The two equations to fulfil in each step are the same for both models, the equilibrium equation and the regularization equation

$$Equilibrium\ equation: \quad \boldsymbol{f_{int}}(\boldsymbol{u}, \tilde{\boldsymbol{u}}) + \boldsymbol{f_{reac_{equi}}} = \boldsymbol{f_{ext}} \tag{3.23}$$

$$Regularization\ equaton: \quad [\boldsymbol{M} + c\boldsymbol{D}(\tilde{\boldsymbol{u}})]\tilde{\boldsymbol{u}} + \boldsymbol{f_{reac_{regu}}} = \boldsymbol{M}\boldsymbol{u} \tag{3.24}$$

but having an internal length variable affects directly affects to the regularization equation. Which now is a nonlinear equation.

The internal forces are calculated like in the original model using a Gauss-Legendre quadrature

$$\boldsymbol{f_{int}}(\boldsymbol{u}, \tilde{\boldsymbol{u}}) = \sum_{p} w_p \sigma_p(\boldsymbol{u}, \tilde{\boldsymbol{u}}) \tag{3.25}$$

but solving the problem now having a nonlinear regularization equation have many implications, which can be firstly seen in the discretization of the diffusion-reaction PDE. Additionally, now the two models with variable internal length have different discretization. For the model with vanishing internal length reduction the discretization leads to

$$\boldsymbol{M} = \int_{\Omega} N^T N \, dV \quad and \quad \boldsymbol{D} = \int_{\Omega} (1 - \mathrm{d}(\tilde{u})) \nabla N^T \nabla N \, dV \tag{3.26}$$

whereas in the model with a bounded internal length reduction is

$$\boldsymbol{M} = \int_{\Omega} N^T N \, dV \quad and \quad \boldsymbol{D} = \int_{\Omega} (1 - \mathrm{ad}(\tilde{u})) \nabla N^T \nabla N \, dV \tag{3.27}$$

in both cases the same mass matrix is obtained but a different diffusion matrix. From now on both models are solved in the same way. The same notation is used and the only difference is that matrix D includes the parameter **a** for the limited internal length reduction case. Where parameter **a** produces further differences between the models it will be denoted.

For both models, the problem has been proposed as a root finding problem using as equations the regularization and the equilibrium error

$$\boldsymbol{r_{equi}} := -\boldsymbol{f_{ext}} + \boldsymbol{f_{int}}(\boldsymbol{u}, \tilde{\boldsymbol{u}}) + \boldsymbol{f_{reac_{equi}}} = 0 \tag{3.28}$$

$$\boldsymbol{r_{regu}} := -\boldsymbol{M}\boldsymbol{u} + [\boldsymbol{M} + c\boldsymbol{D}]\tilde{\boldsymbol{u}} + \boldsymbol{f_{reac_{regu}}} = 0 \tag{3.29}$$

which it can be solved applying the Newton method for nonlinear systems and can the problem can be simplified as

$$\boldsymbol{K}(\boldsymbol{x})\Delta\boldsymbol{x} = \boldsymbol{f} \tag{3.30}$$

and

$$\boldsymbol{K}(\boldsymbol{x})\boldsymbol{\delta x} = \boldsymbol{f} \tag{3.31}$$

where $\Delta\boldsymbol{x}$ or $\delta\boldsymbol{x}$ are the variables that want to be calculated in each step or iteration, that are the same that in the original model: the nonlocal displacements $\tilde{\boldsymbol{u}}$, the local displacements $\boldsymbol{u}$ and the reaction forces of the equilibrium and regularization equation due to the boundary conditions. The matrix $\boldsymbol{K}(\boldsymbol{x})$ does the function of the tangent matrix and as it is not linear, $\boldsymbol{K}(\boldsymbol{x})$ has to be calculated at the start of each step or iteration.

The problem is computed at the step $k + 1$ as

$$\begin{pmatrix} {}^{k}\boldsymbol{K}_{uu} & {}^{k}\boldsymbol{K}_{u\tilde{u}} & \boldsymbol{A}^{T} & 0 \\ \boldsymbol{K}_{\tilde{u}u} & {}^{k}\boldsymbol{K}_{\tilde{u}\tilde{u}} & 0 & \boldsymbol{A}^{T} \\ \boldsymbol{A} & 0 & 0 & 0 \\ 0 & \boldsymbol{A} & 0 & 0 \end{pmatrix} \begin{pmatrix} {}^{k+1}\Delta\boldsymbol{u} \\ {}^{k+1}\Delta\tilde{\boldsymbol{u}} \\ {}^{k+1}\Delta\boldsymbol{\lambda}_{\boldsymbol{equi}} \\ {}^{k+1}\Delta\boldsymbol{\lambda}_{\boldsymbol{regu}} \end{pmatrix} = \begin{pmatrix} -{}^{k}\boldsymbol{r}_{\boldsymbol{equi}} \\ -{}^{k}\boldsymbol{r}_{\boldsymbol{regu}} \\ \boldsymbol{B} \\ \boldsymbol{B} \end{pmatrix} \tag{3.32}$$

where

$${}^{k}\boldsymbol{K}_{uu} = \frac{\partial r_{equi}}{\partial u} = \sum_{p} w_p(1-d_p)E \tag{3.33}$$

$${}^{k}\boldsymbol{K}_{u\tilde{u}} = \frac{\partial r_{equi}}{\partial \tilde{u}} = \sum_{p} w_p E \varepsilon_p \, d'_p \tag{3.34}$$

$$\boldsymbol{K}_{\tilde{u}u} = \frac{\partial r_{regu}}{\partial u} = \boldsymbol{M} \tag{3.35}$$

$${}^{k}\boldsymbol{K}_{\tilde{u}\tilde{u}} = \frac{\partial r_{regu}}{\partial \tilde{u}} = \boldsymbol{M} + c\boldsymbol{D}\left({}^{k}\tilde{\boldsymbol{u}}\right) + c\frac{d\boldsymbol{D}({}^{k}\tilde{\boldsymbol{u}})}{d\tilde{u}}\,{}^{k}\tilde{\boldsymbol{u}} \approx \boldsymbol{M} + c\boldsymbol{D}\left({}^{k}\tilde{\boldsymbol{u}}\right) \tag{3.36}$$

and in each iteration $i+1$ of the step $k+1$ the system to be solve is

$$\begin{pmatrix} {}^{k}\boldsymbol{K}_{uu}{}^{i} & {}^{k}\boldsymbol{K}_{u\tilde{u}}{}^{i} & A^{T} & 0 \\ \boldsymbol{K}_{\tilde{u}u} & {}^{k}\boldsymbol{K}_{\tilde{u}\tilde{u}}{}^{i} & 0 & A^{T} \\ A & 0 & 0 & 0 \\ 0 & A & 0 & 0 \end{pmatrix} \begin{pmatrix} {}^{k+1}\boldsymbol{du}^{i+1} \\ {}^{k+1}\boldsymbol{d\tilde{u}}^{i+1} \\ {}^{k+1}\boldsymbol{d\lambda_{equi}}^{i+1} \\ {}^{k+1}\boldsymbol{d\lambda_{regu}}^{i+1} \end{pmatrix} = \begin{pmatrix} {}^{k}-\boldsymbol{r_{equi}}^{i} \\ {}^{k}-\boldsymbol{r_{regu}}^{i} \\ 0 \\ 0 \end{pmatrix} \tag{3.37}$$

where

$${}^{k}\boldsymbol{K}_{uu}{}^{i} = \frac{\partial r_{equi}}{\partial u} = \sum_{p} w_p(1-d_p)E \tag{3.38}$$

$${}^{k}\boldsymbol{K}_{u\tilde{u}}{}^{i} = \frac{\partial r_{equi}}{\partial \tilde{u}} = \sum_{p} w_p E \varepsilon_p \, d'_p \tag{3.39}$$

$$\boldsymbol{K}_{\tilde{u}u} = \frac{\partial r_{regu}}{\partial u} = \boldsymbol{M} \tag{3.40}$$

$${}^{k}\boldsymbol{K}_{\tilde{u}\tilde{u}}{}^{i} = \frac{\partial r_{regu}}{\partial \tilde{u}} = \boldsymbol{M} + c\boldsymbol{D}\left({}^{k}\tilde{\boldsymbol{u}}^{i}\right) + c\frac{d\boldsymbol{D}({}^{k}\tilde{\boldsymbol{u}}^{i})}{d\tilde{u}}\,{}^{k}\tilde{\boldsymbol{u}}^{i} \approx {}^{k}\boldsymbol{K}_{\tilde{u}\tilde{u}} = \boldsymbol{M} + c\boldsymbol{D}({}^{k}\tilde{\boldsymbol{u}}) \tag{3.41}$$

and the variables are computed as

$${}^{k+1}\boldsymbol{u} = {}^{k}\boldsymbol{u} + {}^{k+1}\Delta\boldsymbol{u} + {}^{k+1}\boldsymbol{du}^{i} \tag{3.42}$$

$${}^{k+1}\tilde{\boldsymbol{u}} = {}^{k}\tilde{\boldsymbol{u}} + {}^{k+1}\Delta\tilde{\boldsymbol{u}} + {}^{k+1}\boldsymbol{d\tilde{u}}^{i} \tag{3.43}$$

$${}^{k+1}\boldsymbol{\lambda_{equi}} = {}^{k}\boldsymbol{\lambda_{equi}} + {}^{k+1}\Delta\boldsymbol{\lambda_{equi}} + {}^{k+1}\mathbf{d}\boldsymbol{\lambda_{equi}}{}^{i} \tag{3.44}$$

$$^{k+1}\boldsymbol{\lambda}_{\boldsymbol{regu}} = {}^{k}\boldsymbol{\lambda}_{\boldsymbol{regu}} + {}^{k+1}\Delta\boldsymbol{\lambda}_{\boldsymbol{regu}} + {}^{k+1}\boldsymbol{d\lambda}_{\boldsymbol{regu}}{}^{i} \tag{3.45}$$

The reason on approximating the calculation of ${}^{k}\boldsymbol{K}_{\tilde{u}\tilde{u}}$ and ${}^{k}\boldsymbol{K}_{\tilde{u}\tilde{u}}{}^{i}$ is discussed in Annex C: Approximated values The control of errors is done as in the original model using a (a) relative error in displacement and in (b) forces and imposing that it should always be below a chosen threshold. But now as the regularization equation is not linear, the error in it is not zero anymore for all iterations and an (c) error control over the regularization equation is needed, even more after approximating the matrix ${}^{k}\boldsymbol{K}_{\tilde{u}\tilde{u}}$ and ${}^{k}\boldsymbol{K}_{\tilde{u}\tilde{u}}{}^{i}$. So, the three relative errors to be controlled are

$$(a)\ tol_u > \frac{\left\| {}^{k+1}\boldsymbol{du}^{i} \right\|}{\left\| {}^{k}\boldsymbol{u} + {}^{k+1}\Delta\boldsymbol{u} \right\|} \tag{3.46}$$

$$(b)\ tol_{equi} > \frac{\left\| \boldsymbol{r}_{\boldsymbol{equi}} \right\|}{\left\| \boldsymbol{f}_{\boldsymbol{reac}_{\boldsymbol{equi}}} \right\|} \tag{3.47}$$

$$(c)\ tol_{regu} > \frac{\left\| \boldsymbol{r}_{\boldsymbol{regu}} \right\|}{\left\| \boldsymbol{f}_{\boldsymbol{reac}_{\boldsymbol{regu}}} \right\|} \tag{3.48}$$

Fourth chapter

4 COMPARISON OF MODELS

The aim of this chapter is to compare the different behaviours of the models between them and test the goodness of the new models regarding the spatial and time mesh size. Additionally, different tests are going to be carried out to know how each parameter of the models ($a, c, \varepsilon_i, \varepsilon_u$, number of weak elements…) affects to each model.

4.1 BEHAVIOUR DESCRIBED BY THE MODELS.

Figure 13 and *figure 14* has been plot using a c value of 5 mm^2, 320 elements, a equal to 0.9 and the original values of the problem presented above.

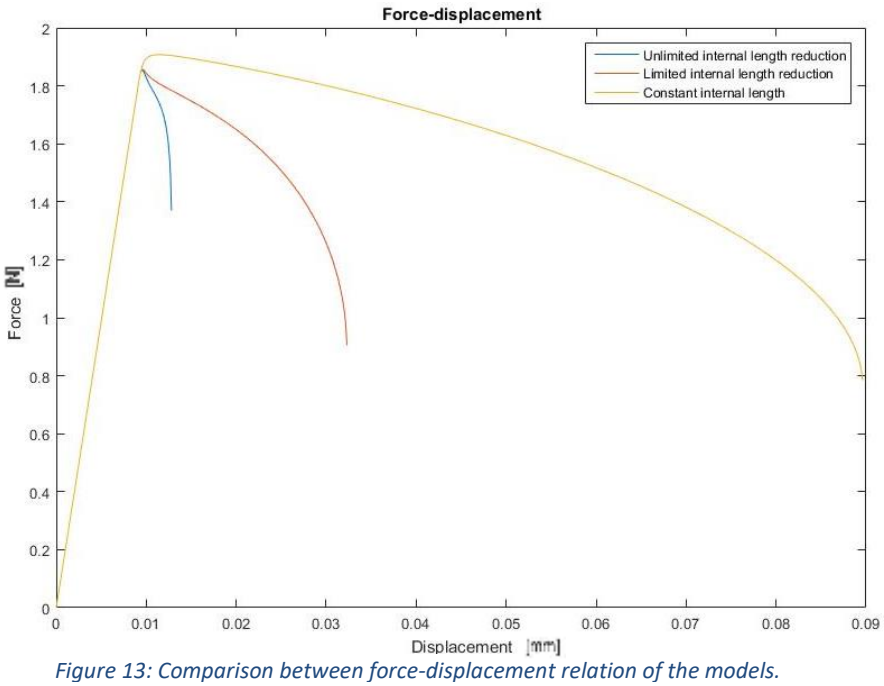

Figure 13: Comparison between force-displacement relation of the models.

Figure 13 shows the expected behaviour from the models presented. More ductile behaviour when the internal length is not reduced and a more fragile behaviour when the internal length reduction is not limited. Just to emphasise it, the plot force-displacement shows how the **fracture energy**, energy needed to form a fissure in a material which can be interpreted as the area formed by the curve force-displacement and the abscissa axis, is less in the new models than in the original one.

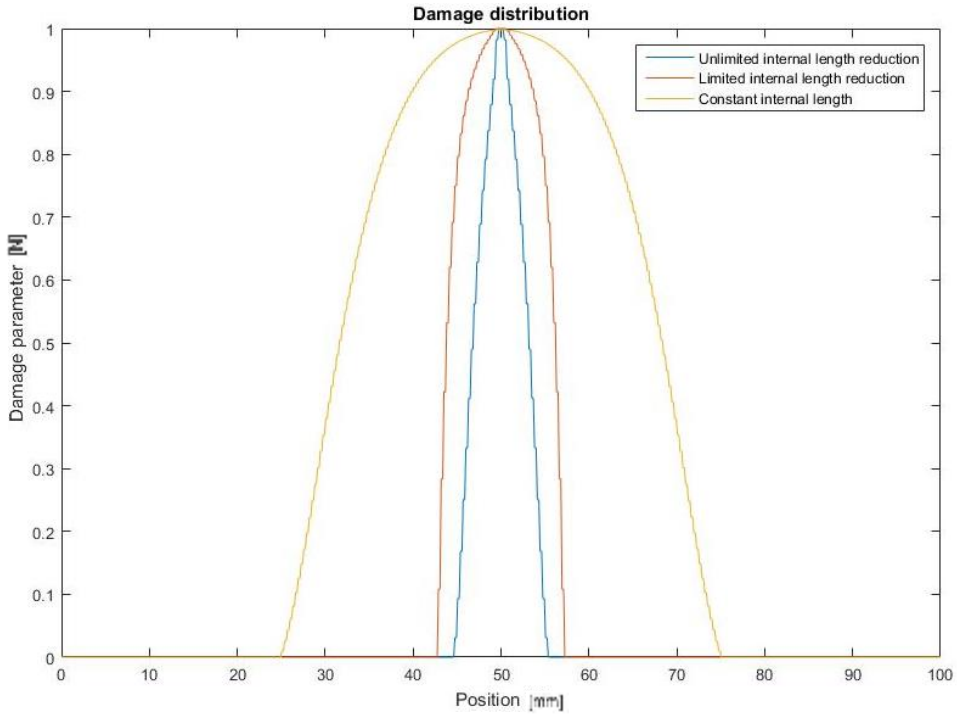

Figure 14: Comparison of damage distribution in the last step of the problem for all models.

A higher energy fracture needed can be translated as more damage supported by the elements of the beam and as the damage cap is the same for all three models the damage must be more distributed over the beam. A more width damage distribution for more ductile behaviour as seen in *figure 14*.

4.2 GOODNESS OF THE MODELS.

One of the most important thing for any model is to check that a is non-mesh size dependant for the spatial and the time mesh. When the original model was presented back in 2005 the authors already did test the spatial mesh dependence, but as this is an academic project it has been reproduced again.

For all three models, different mesh sizes (40, 80, 160, 320 and 640 elements) are tested aiming for a convergence of the results when the mesh gets finer. The c value used is 5 mm^2 and a is 0.9.

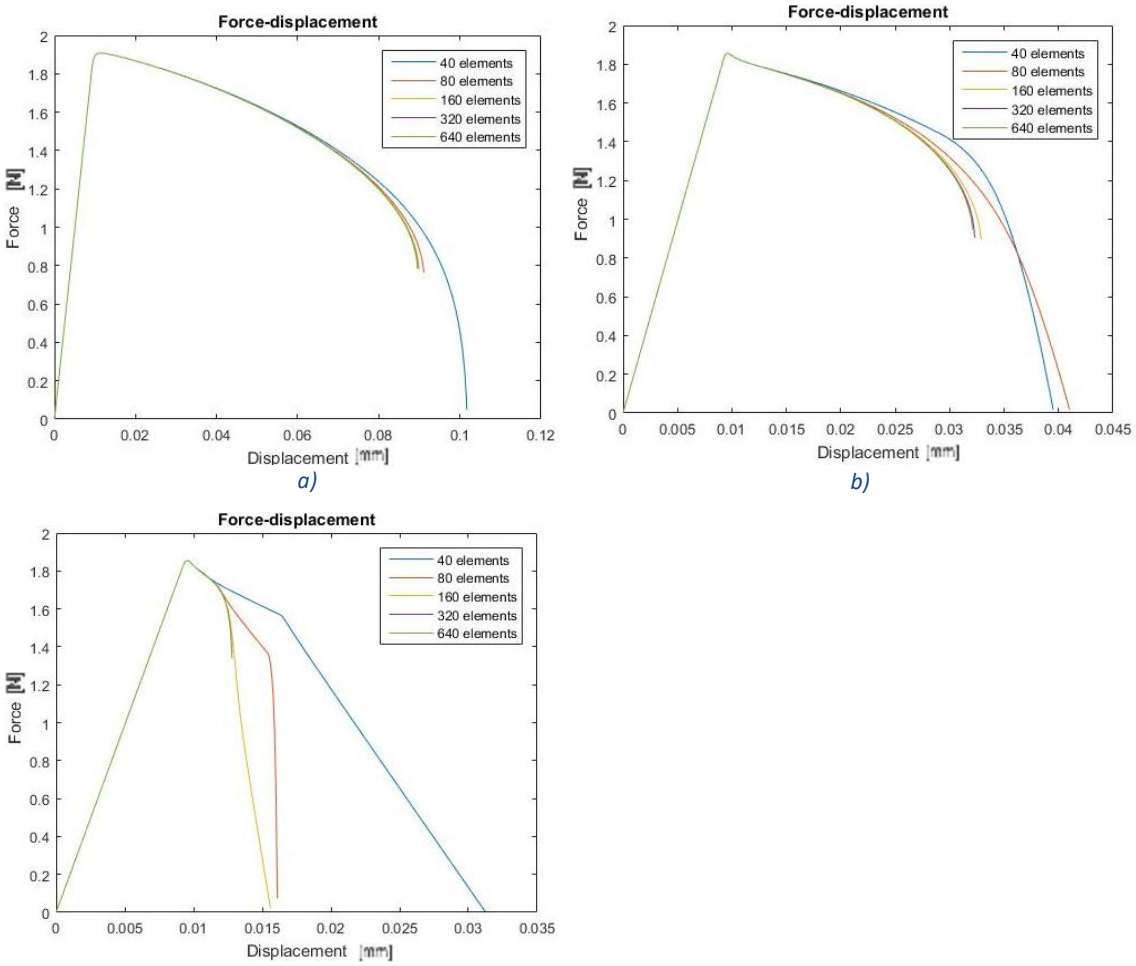

Figure 15: Force-displacement charts with variable spatial mesh size. a) Original model. b) New model limited internal length reduction. c) New model nonlimited internal length reduction.

All three models converge to a unique solution when the spatial mesh gets finer proving their spatial mesh size independence in the force-displacement relation and in damage distribution.

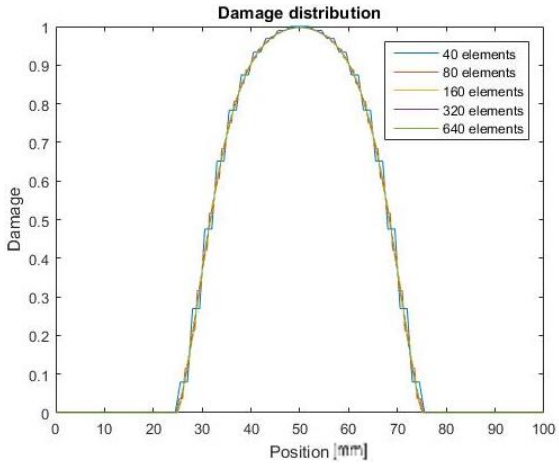

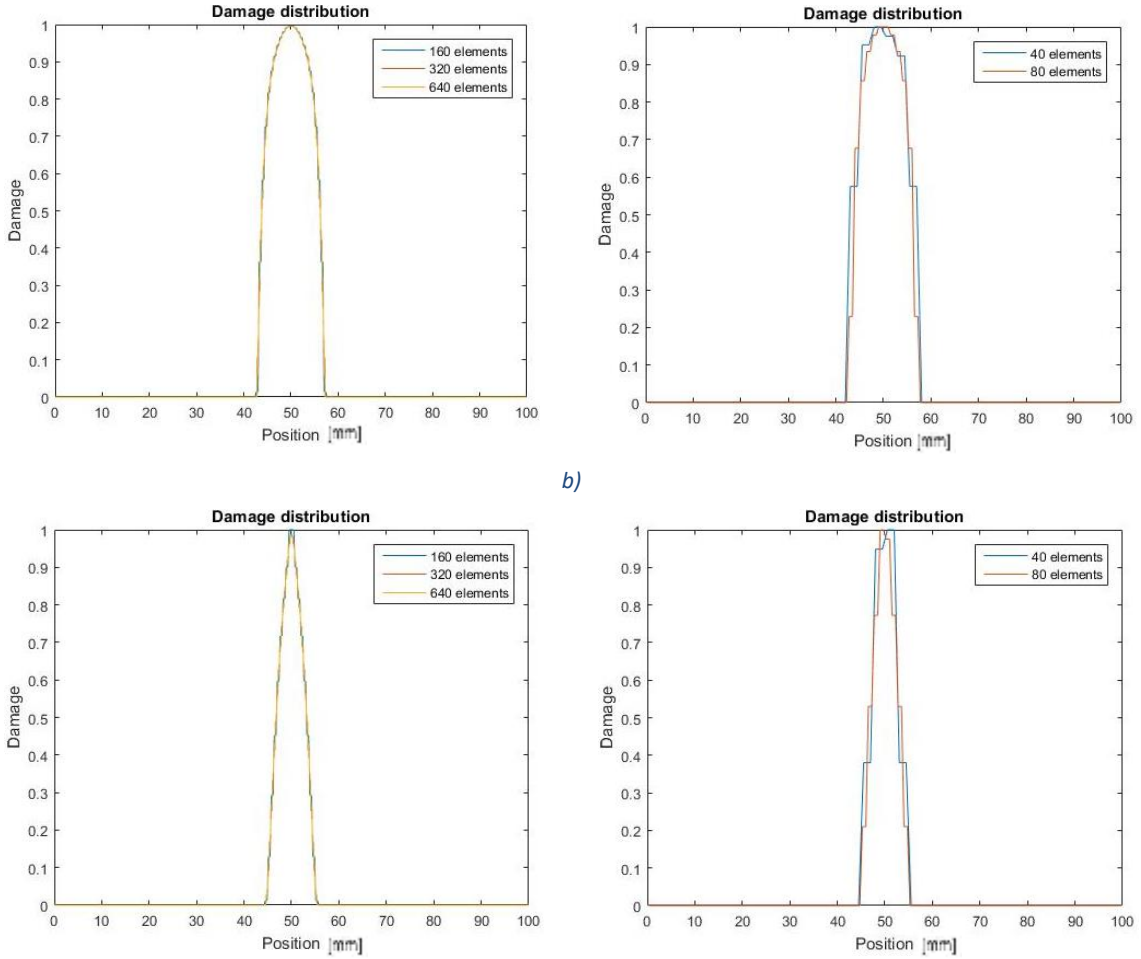

Figure 16: Damage distribution charts of the last step of the problem with variable spatial mesh size. a) Original model. b) New model with limited internal length reduction. c) New model with nonlimited internal length reduction.

For the new models the damage distribution for the cases with 40 and 80 elements have been presented in a different plot because they present an asymmetry in the damage distribution which is not acceptable for this problem.

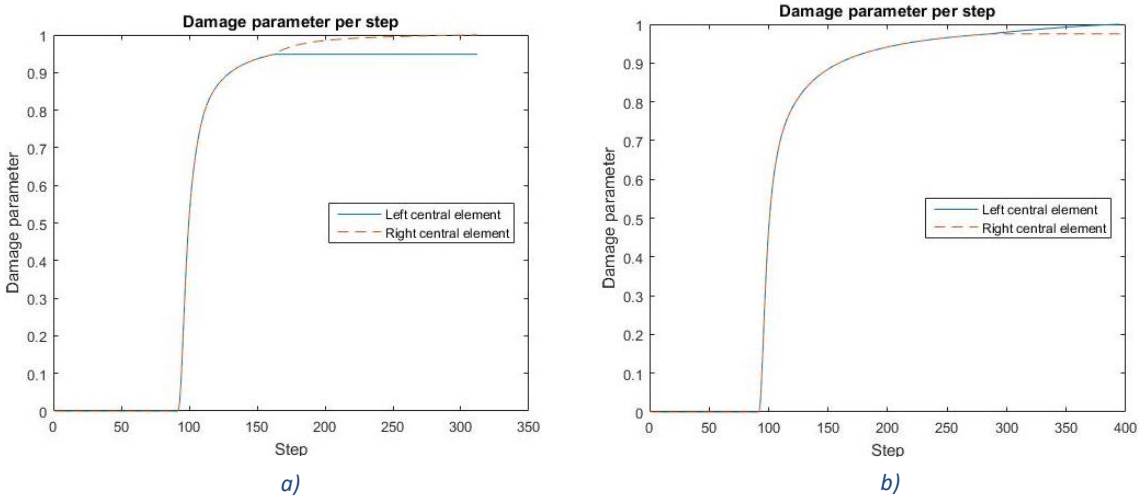

Figure 17: Display of the asymmetry on damage in the new models with 40 elements. a) Nonlimited internal length reduction. b) Limited internal length reduction.

This asymmetry is due to an error accumulation in one of the two central elements for not using a finer spatial mesh enough which is increased due to the reduction of the internal length in the more damaged elements as *figure 17* shows, calculated using 40 elements an initial c value of 5 mm^2 and a equal to 0.9. As the original model do not concentrated damage in the already damage zones the possible error happening when running the model get compensated due to a constant c value during all the problem.

Moreover, the time independence of the models has been tested, for this problem as there is no time related variables, the prescribed displacement for each step does the function of the time step. Different displacement steps (1e-3, 1e-4, 1e-5, 1e-6, 1e-7 mm), with 320 elements, a c value of 5 mm^2 and a equal to 0.9 has been used for *figure 18* and *figure 19*.

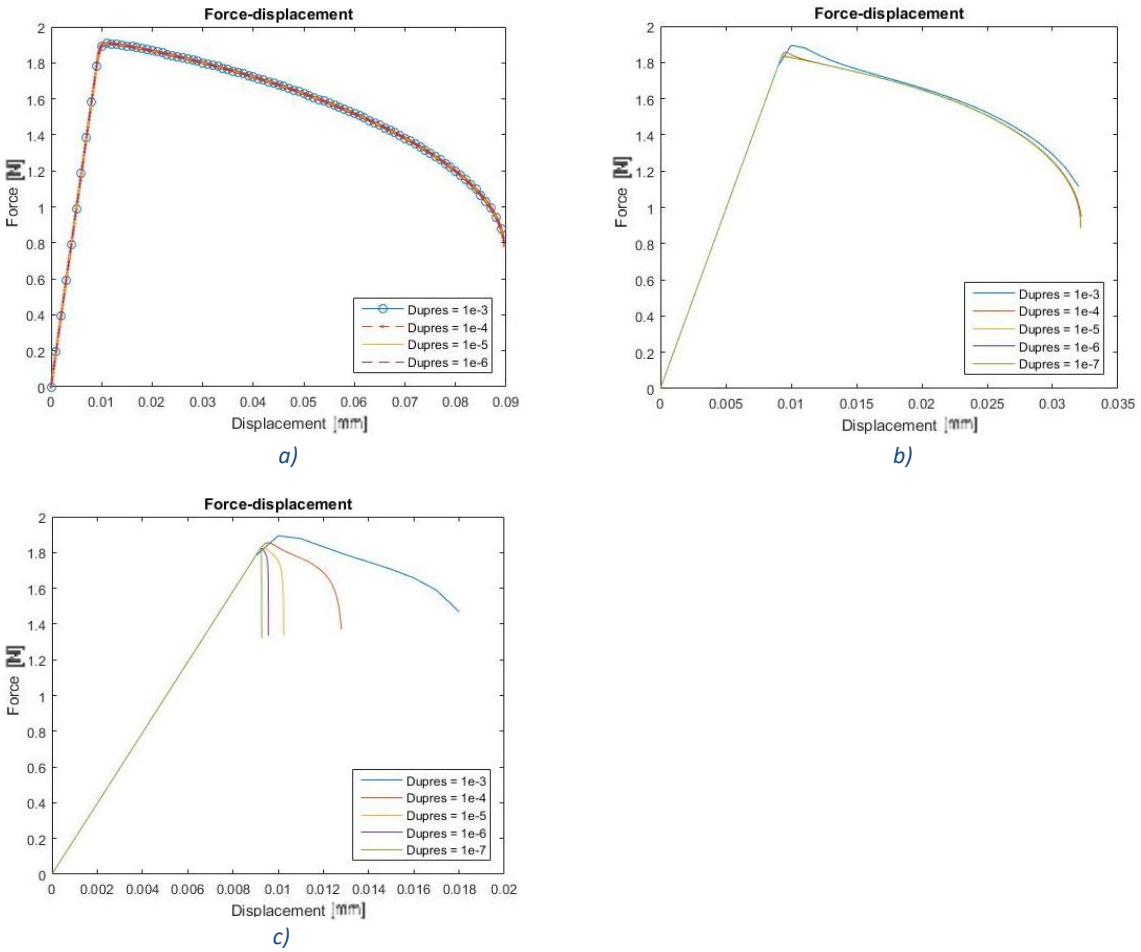

Figure 18: Force-displacement charts with variable time mesh size. a) Original model. b) New model limited internal length reduction. c) New model nonlimited internal length reduction.

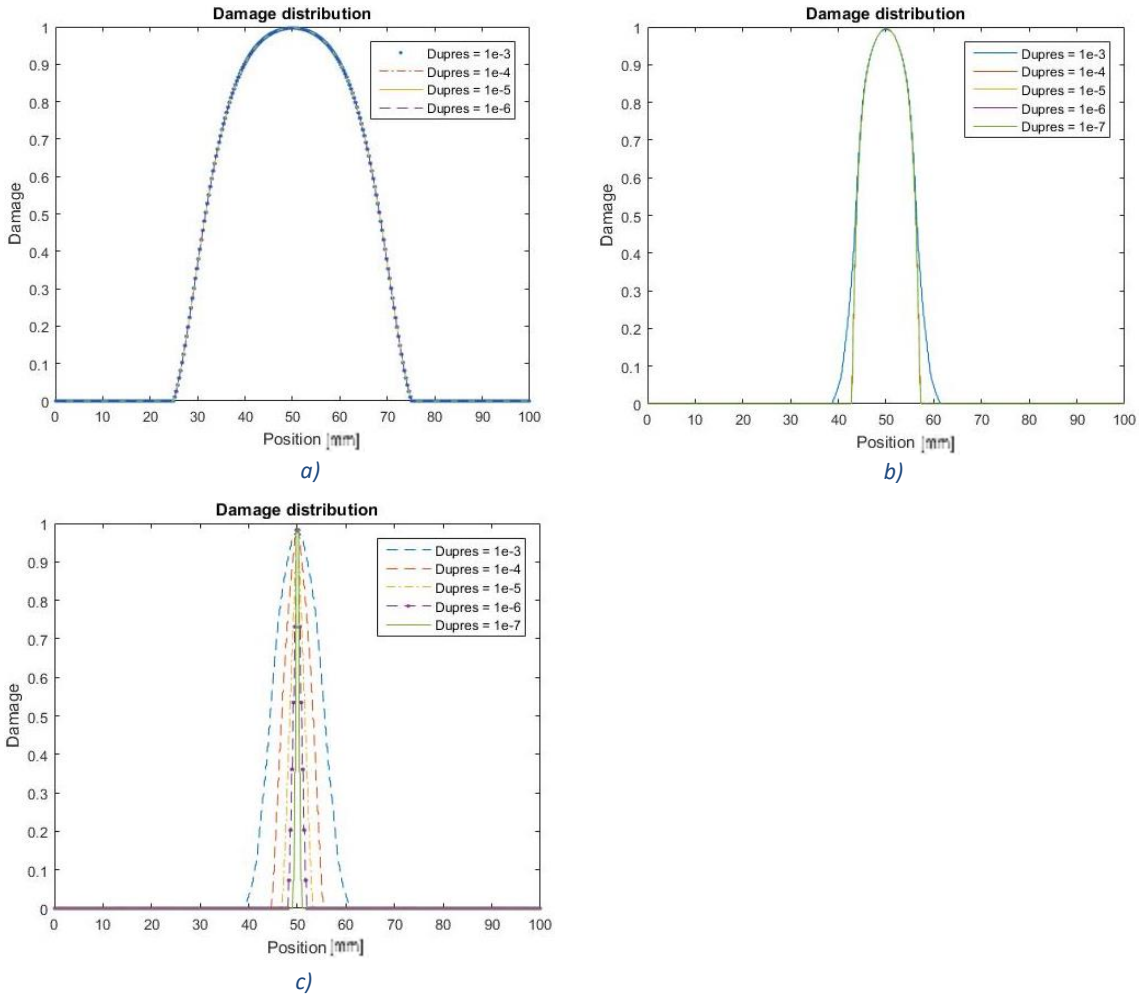

Figure 19: Damage distribution charts of the last step of the problem with variable time mesh size. a) Original model. b) New model with limited internal length reduction. c) New model with nonlimited internal length reduction.

The original model and the model with a bounded internal length reduction present a time mesh size independence, whereas the model with a vanishing internal length displays a pathologic dependence on the time step size, affecting directly to the width of the damaged zone in the last step and for instance to the response of the beam, for instance making the beam more brittle when the time mesh gets finer.

4.3 PARAMETER EFFECT ON MODELS.

In the paper presented in 2005 some parameters were tested changing its value and seeing the effects of them in the model. For this dissertation, the parameters tested in the original paper and some are going to be tested to see its effects on the models. Firstly, starting with a variable value of c (1, 2, 5, 10 mm), with 320 elements, $a = 0.9$ and the rest of the original values of the problem *figure 20* and *figure 21* can be obtained.

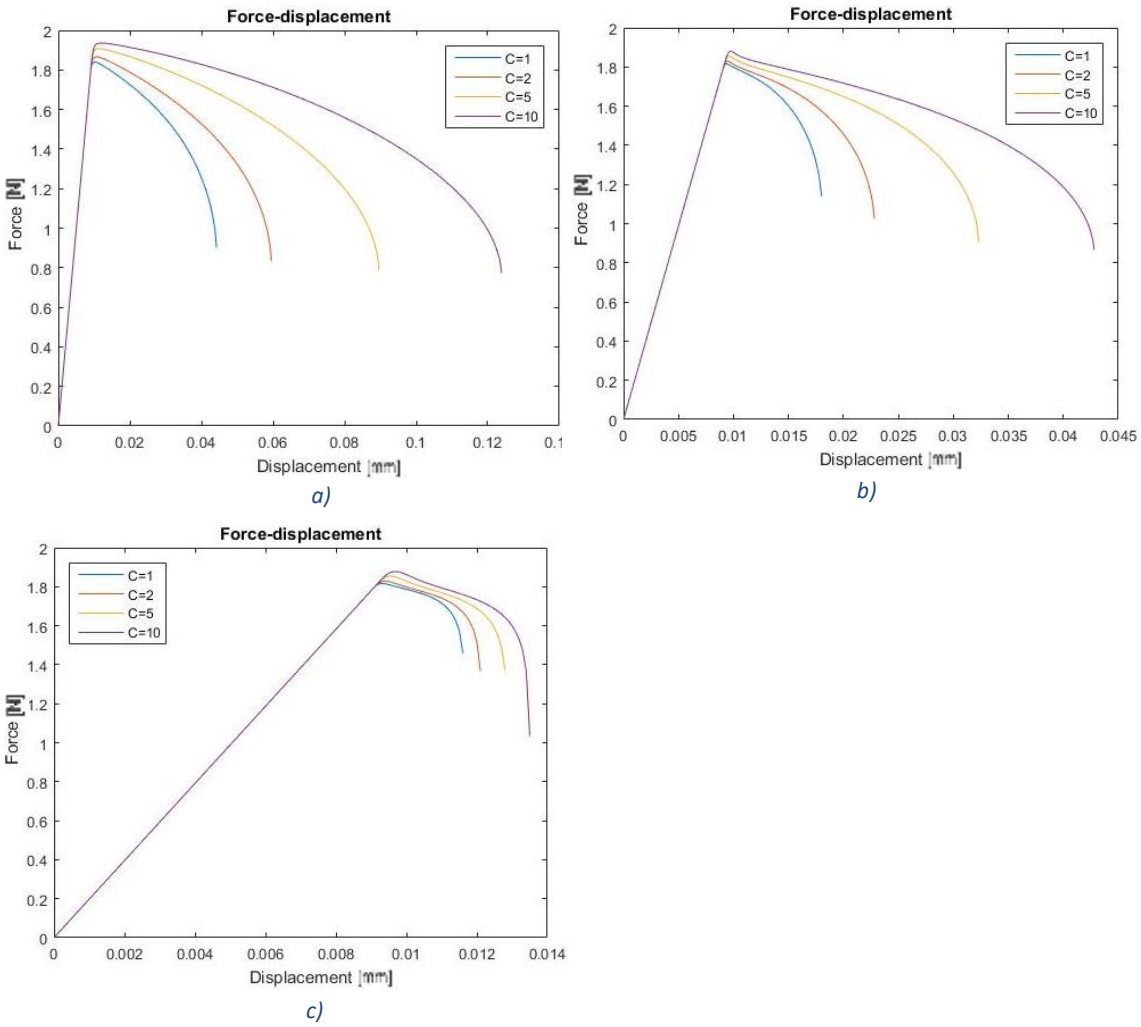

Figure 20: Force-displacement charts with variable initial internal length value. a) Original model. b) New model limited internal length reduction. c) New model nonlimited internal length reduction.

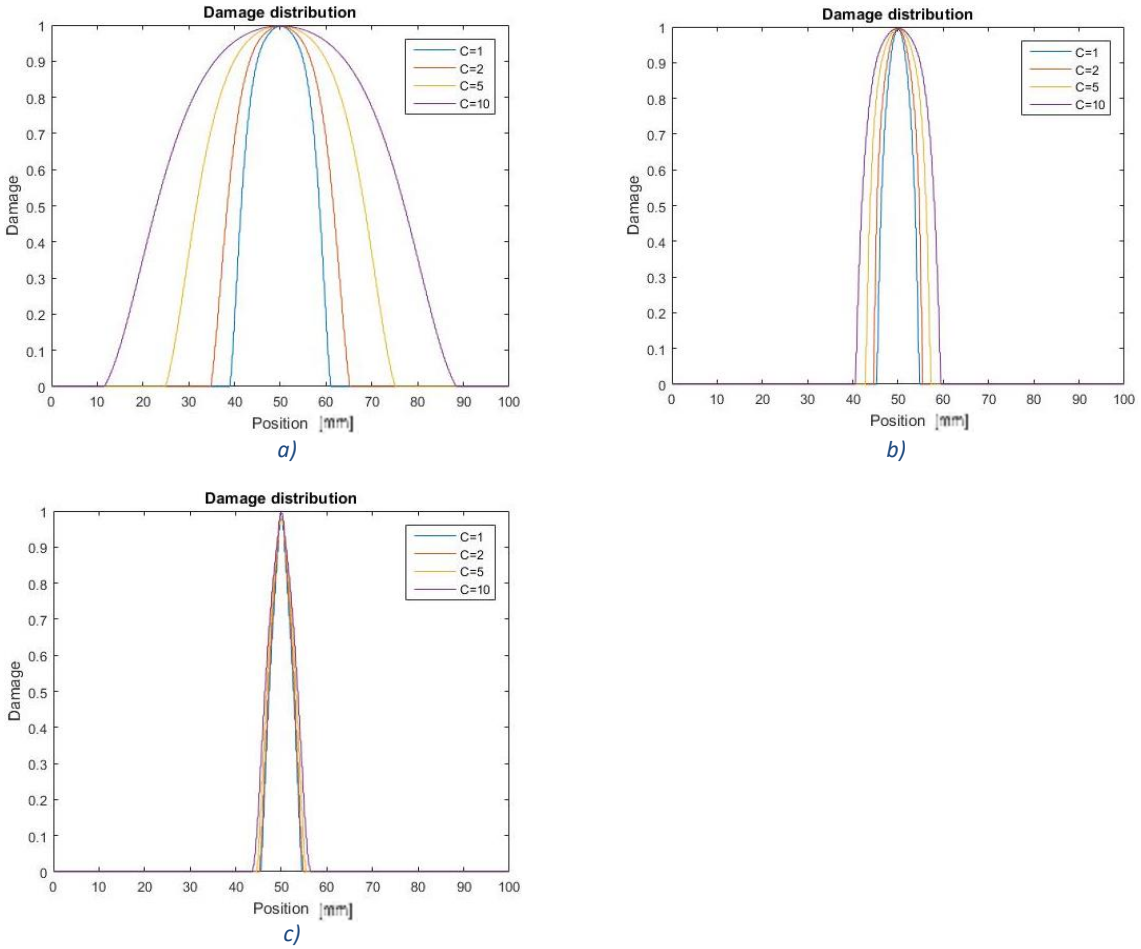

Figure 21: Damage distribution charts of the last step of the problem with variable initial internal length value. a) Original model. b) New model with limited internal length reduction. c) New model with nonlimited internal length reduction.

The effect of the internal length c chosen on the original is way more significant than in the two new models. Having its value reduced with damage in the new models makes the initial c value less important. Even though, the model with a limited internal length reduction as there is always a minimum value of c (10% in this problem with $a = 0.9$) the effect on the behaviour is slightly higher compared to the other new model. What can be concluded from that is that making a good choice of c is very important if someone uses the original model or the new model with a limited internal length reduction, whereas if the other new model is used making a good choice of c is less important.

Another interesting parameter to test is the number of weakened elements, in the original problem always a 10% of weakened elements have been used. But, in order to know its effect different percentage of weakened elements (5%, 10%, 30%, 50%) have been used for the same problem with 320 number of total elements, a c value of 5 with $a = 0.9$.

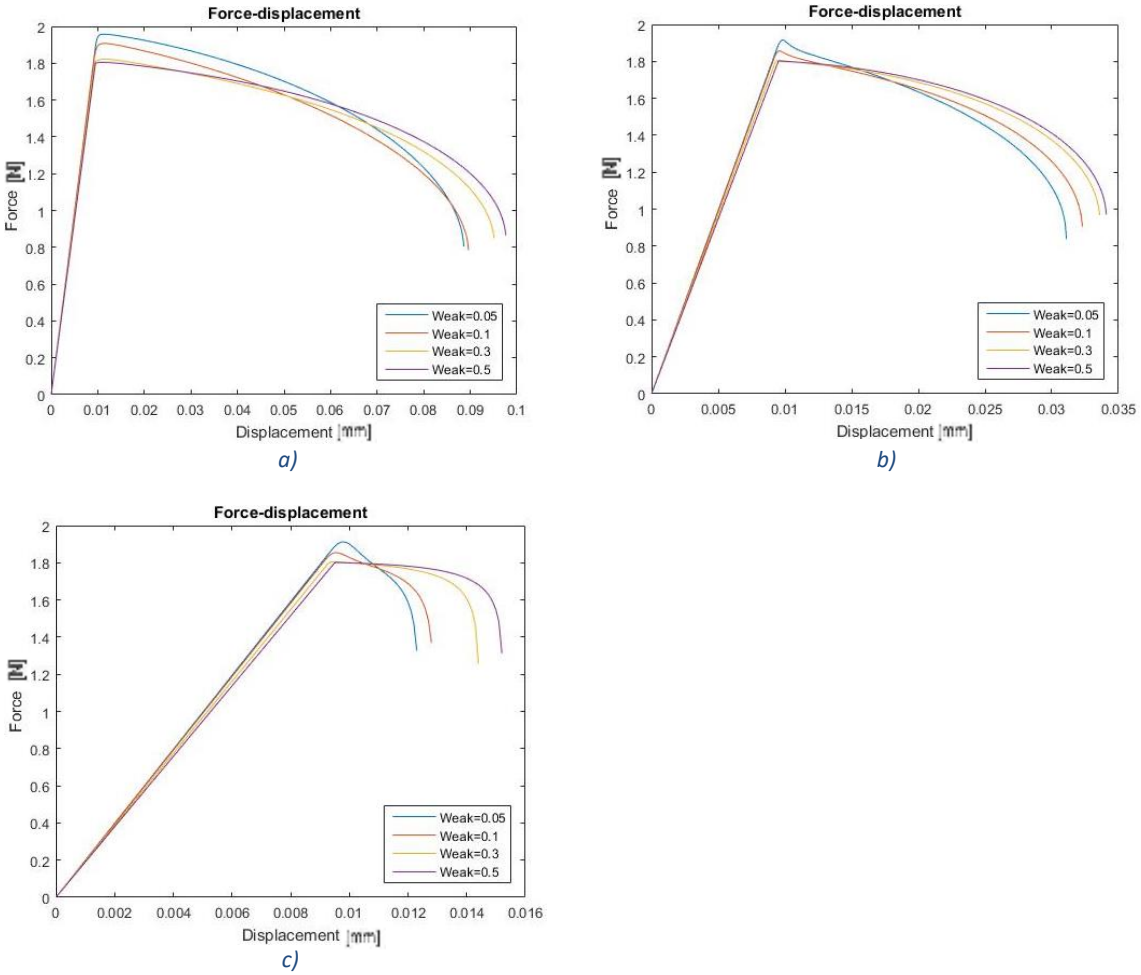

Figure 22: Force-displacement charts with variable number of weakened elements. a) Original model. b) New model limited internal length reduction. c) New model nonlimited internal length reduction.

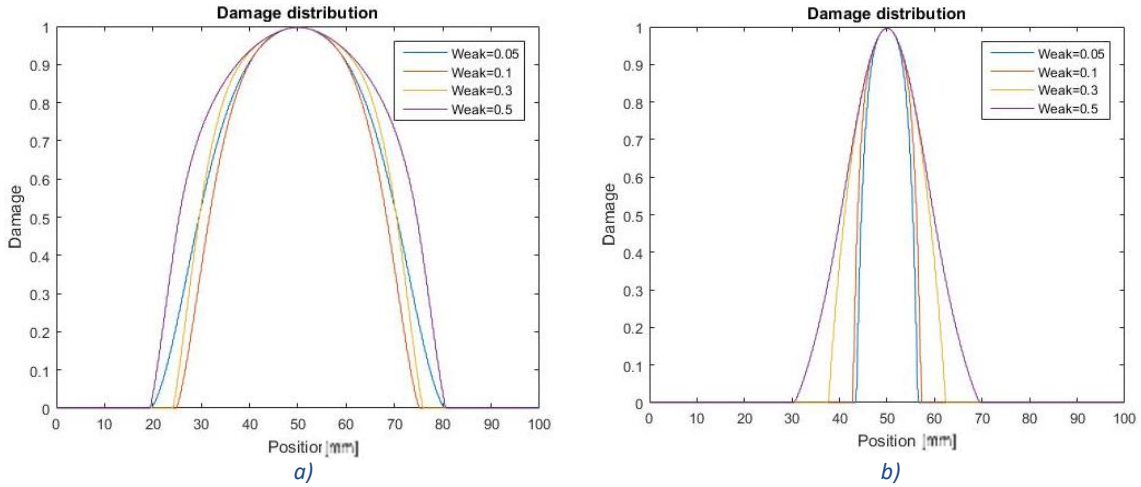

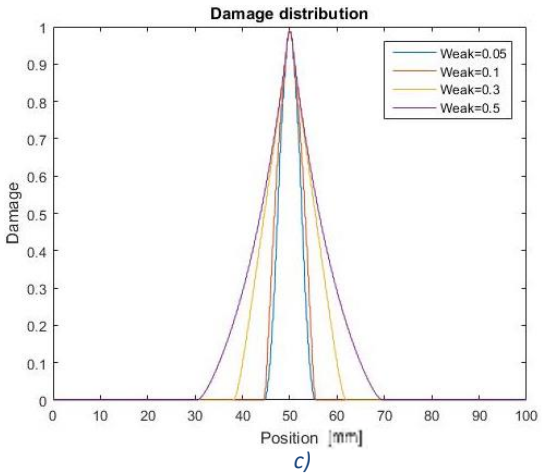

c)

Figure 23: Damage distribution charts of the last step of the problem with variable number of weakened elements. a) Original model. b) New model with limited internal length reduction. c) New model with nonlimited internal length reduction.

Figure 22 and *figure 23* at first look show an illogical behaviour by the models. Displaying a more fragile behaviour for the problems with the less number of weakened elements in all three models. The reason behind this is that in the two new models damage concentrates in the already damaged zones and as the weakened zone gets thinner the starting damage zone in the first nonlinear steps gets also thinner producing a higher concentration in the central elements of the beam and exhibiting a more fragile behaviour for those cases. However, the original model which does not have this damage concentration behaviour, but the most fragile behaviour is displayed by the problem with less weakened elements.

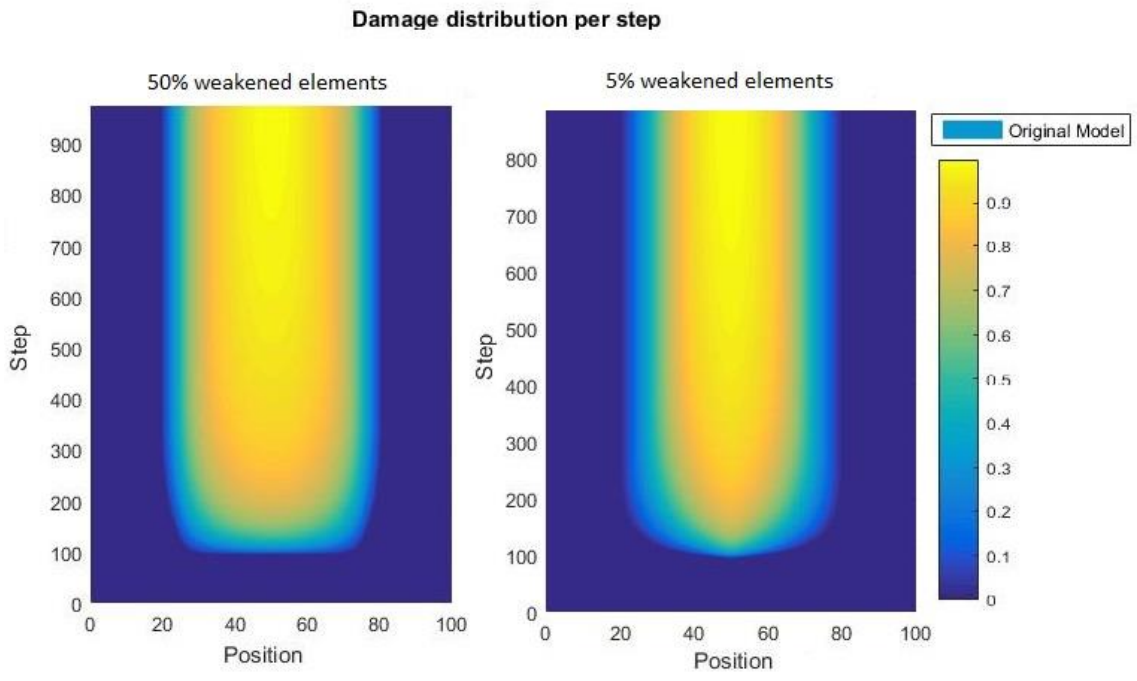

Figure 24: Damage per step in the original model with 5% and 50% weakened elements comparison.

The reason behind it is shown in *figure 24* which shows that the initial elements damaged is thinner for the less weakened elements and even though there is no damage concentration in this model having a reduced Young's modulus in less elements makes that the deformation concentrates more on them, producing a faster increase on damage on these elements.

Another option that raised during the time working on this project, is the effect of the central elements weaken. Not reducing its Young's modulus but reducing the lower bound threshold deformation ε_i for the damage effect in order to know the influence of the Young's modulus and the lower bound threshold. So, the same problem has been tested with different conditions. In one case, the weakened elements have a 10% reduction on the Young's modulus and in the other case is the lower bound threshold that has a 10% reduction in the weakened elements.

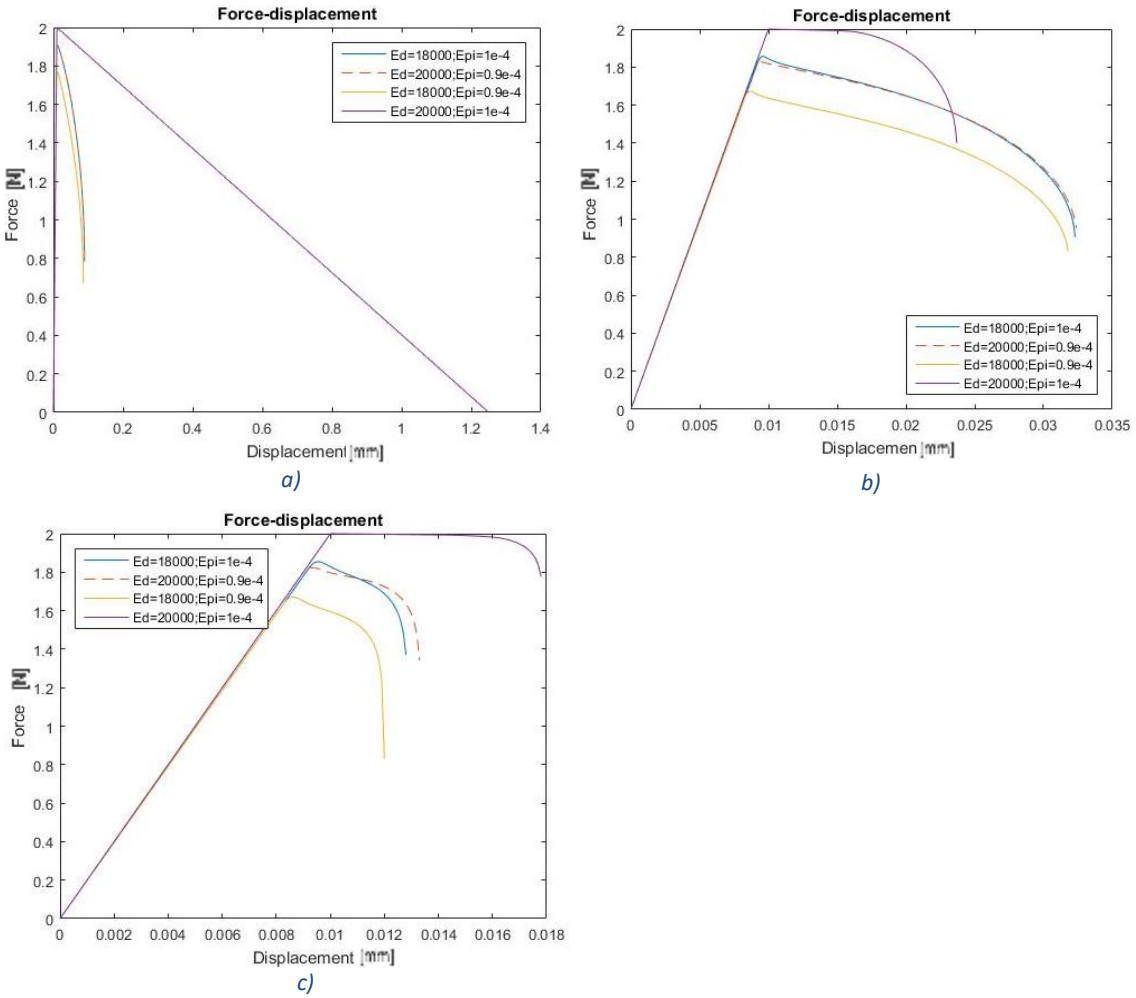

Figure 25: Force-displacement charts with variable weaken conditions. a) Original model. b) New model limited internal length reduction. c) New model nonlimited internal length reduction.

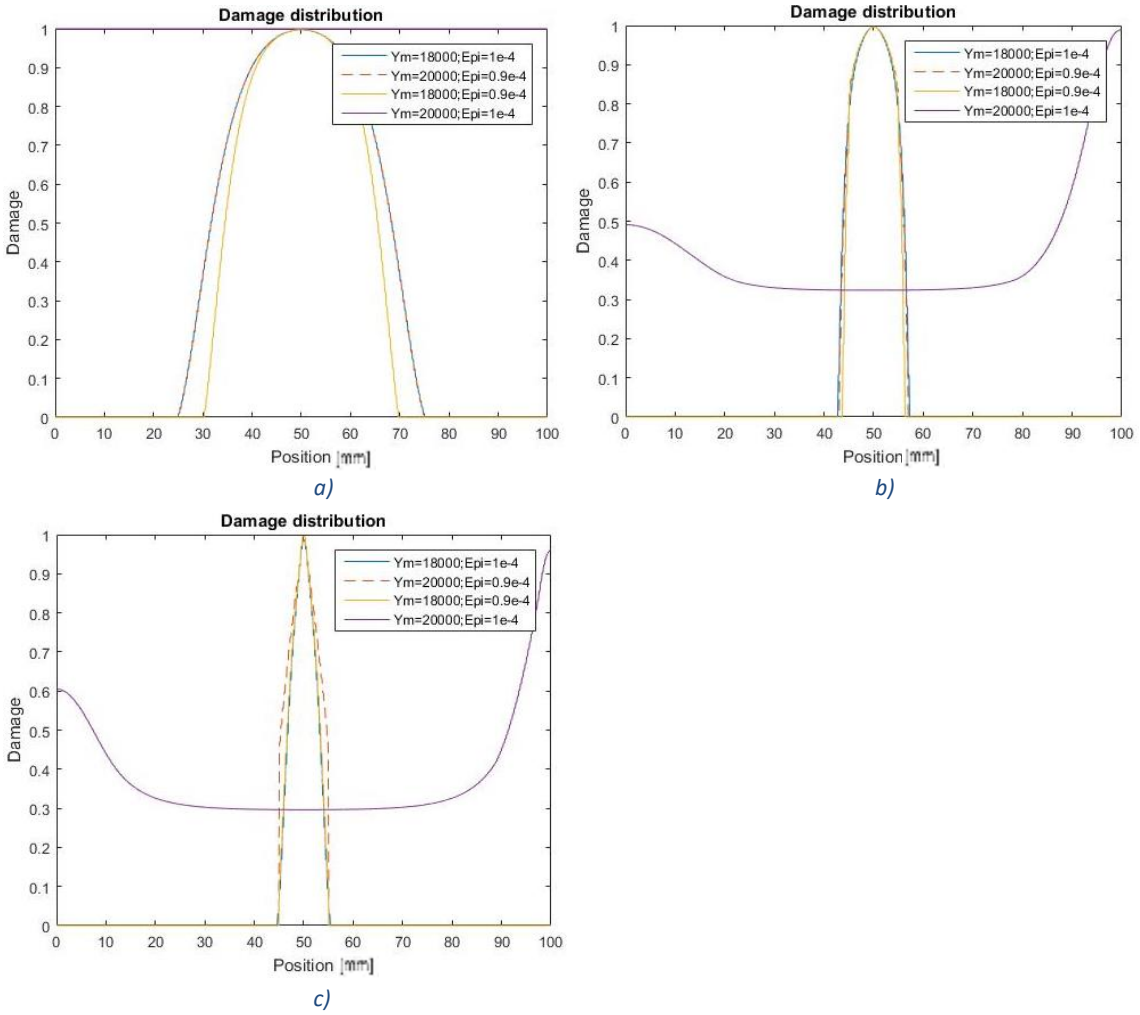

Figure 26: Damage distribution charts of the last step of the problem with variable weaken conditions. a) Original model. b) New model with limited internal length reduction. c) New model with nonlimited internal length reduction.

There are many things to comment about *figure 25* and *figure 26*, first of all in all models changing from reducing the Young's modulus by a 10% to reducing lower bound damage threshold by the same amount does not make big changes on the overall behaviour of the models.

Another thing that seems to happen is that the new model with nonlimited internal length reduction cannot go outside of the weakened elements when having the same Young's modulus for all the beam but the weaken elements having a reduced lower bound damage threshold, *figure 26.c.* The slope of damage described is a straight vertical line meaning that the model chooses to only damage elements that are already damaged. To check that, the damage distribution per step with the conditions just mentioned ($E = 20000$ and $\varepsilon_i = 0.9e - 10$) is shown in *figure 27*.

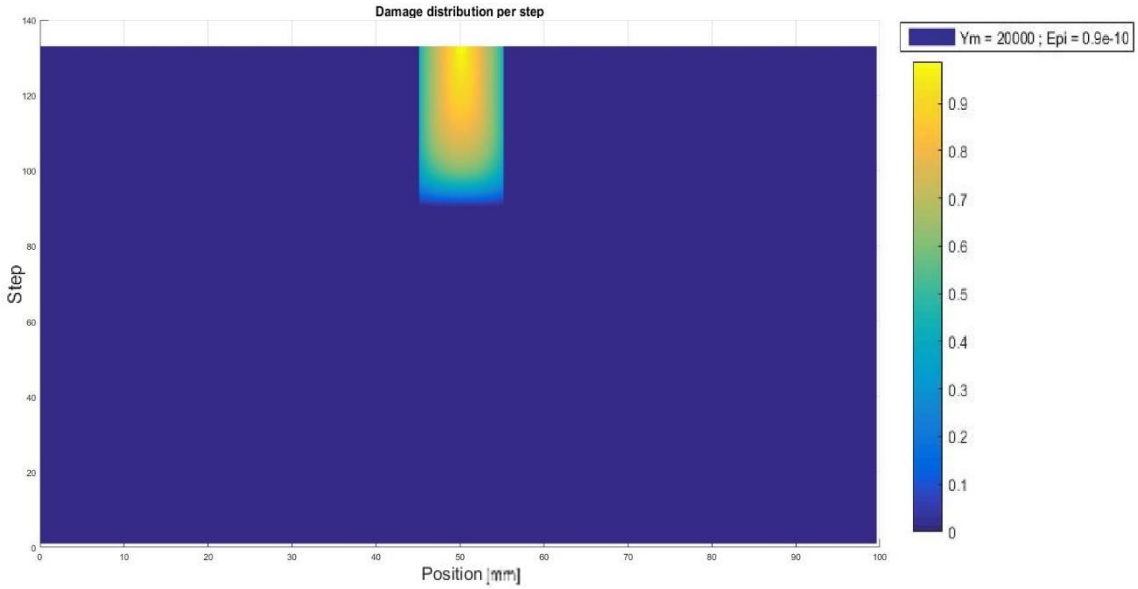

Figure 27: Damage distribution per step for the new model with unbounded internal length reduction. Using as weaken conditions the reduction of the lower bound threshold of damage.

The last thing to comment about the previous figures shown and about the parameters effects on the problem is that looking at *figure 25* and *figure 26* it can be seen that even though in the cases using a uniform beam composition, meaning no weakened elements or weakened elements with the same conditions than the rest of the elements, the behaviour described by the two new models do not describe a homogeneous response. In those figures, it can be clearly see how the damage concentrates on the start and the end of the beam and that the force-displacement charts do not describe a linear softening behaviour for the new models with homogeneous conditions.

Investigating further on this problem the reason behind it is shown in *figure 28*.

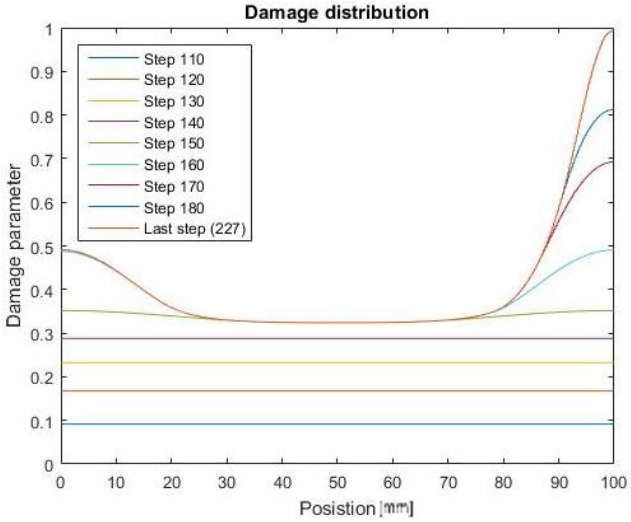

Figure 28: Damage distribution showing the error on homogeneous materials.

Figure 28 shows how a small error in calculations is enhanced due to the internal length reduction in damaged zones and are the reason behind the concentration of damage on the extreme elements of the beam.

This same problem on modelling homogeneous materials can happen on physical laboratory test, where having a totally homogeneous material is really difficult and can lead to the same problem just exposed.

The last parameter to be discussed in this dissertation is the threshold parameter a for the new model with a bounded internal length reduction. The following charts have been calculated with 320 elements, c equal to 5 mm^2 and the rest of the values of the problem presented in *table 5*.

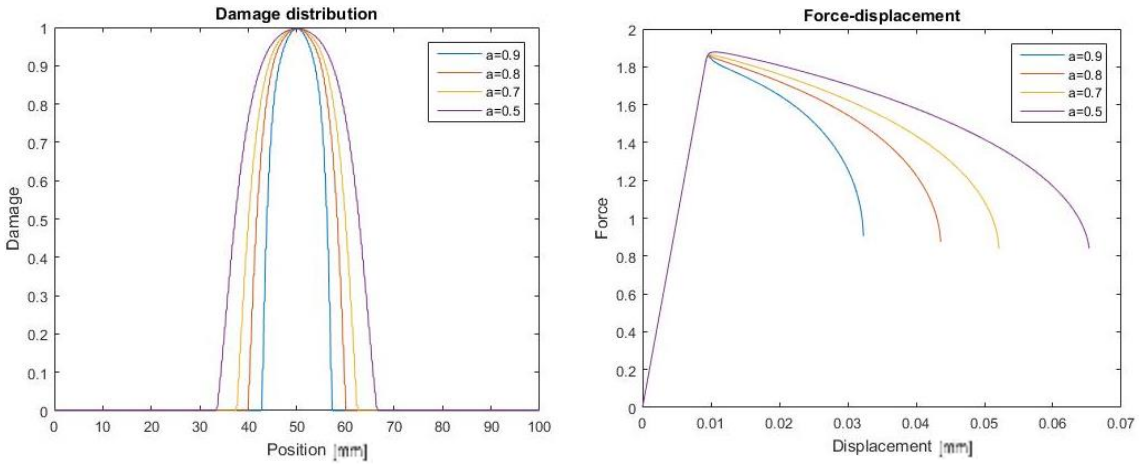

a) *b)*

Figure 29: New model with a bounded internal length reduction with a variable parameter a. a) Damage distribution. b) Force-displacement behaviour.

The parameter a in this new model has a similar effect as the initial internal length value c. Affecting the ductility of the model. For lower values of a, meaning higher minimum internal length values, characterize a more ductile behaviour.

Fifth chapter

5 CONCLUSIONS AND FUTURE WORK

5.1 CONCLUSIONS

Through this dissertation two new finite element methods to process fracture in semi brittle materials have been presented. Both models are pretty similar but the unique different between them (including a threshold for the internal length reduction) results in very different outcomes. There are three main things that should be remarked of this dissertation:

1. **Introducing a variable internal length.** This was the main objective of all the work. Both models presented in chapter 3 work with a variable internal length and show the expected results of them.
2. **Model with vanishing internal length.** This model presents a pathological dependency on the temporal mesh size. Meaning that its results should be mistrust.
3. **Model with bounded internal length reduction.** This model presents independence of the temporal and spatial mesh size used. Thus, it can be used with certainty of the results obtained.
4. **Bounded new model and original model comparison.** The new model with a variable internal length and a bounded diffusion reduction present a more brittle response compared to the results obtained with the original model.
5. **Variable dependence.** In the new model with a bounded internal length reduction two parameters must be determined in order to obtain the behaviour wanted. These parameters are: the initial internal length c and parameter α that determinates the final internal length value. Both of them affect to the ductility of the model, a higher value of c and a lower value of α leads to a less fragile behaviour.

5.2 FUTURE WORK

From the work presented in this dissertation the main objective in the near future should be centred around the model with a limited internal length reduction, because do not present a pathological dependence of the temporal mesh size. Some directions to be discussed in the future could be:

- **Implementation of the model in 2D and 3D.** The model presented has only been implemented to work in one dimension, but from the results obtained implementing this model in two dimensions and even in three dimensions could be an interesting research direction.
- **Simulation of brittle fracture.** An interesting direction of research would be testing this new model with a non-vanishing internal length on real materials and see if it models brittle fracture with accuracy.
- **Identification of parameters a and c.** The new model behaviour depends on two parameters (a, c) that have to be chosen depending on what type of material or response is being modelled. Investigating on how to identify these parameters easily could be another direction of research.

ANNEX A: WEAK FORM DISCRETIZATION

In this appendix is developed how the weak form is obtained from the strong for all three models.

ORIGINAL MODEL

The strong form of this model is

$$\tilde{u} - c\nabla^2\tilde{u} = u \; in \; \Omega \tag{A.1}$$

$$\tilde{u}(x) = u(x) \qquad on \; \partial\Omega \tag{A.2}$$

applying this to our one dimension problem the strong form remains as

$$\tilde{u} - c\frac{\mathrm{d}}{\mathrm{dx}}\left[\frac{d\tilde{u}}{dx}\right] = u \quad on \; x \in (0, l) \tag{A.3}$$

$$\begin{cases} \tilde{u}(0) = u(0) = 0 \\ \tilde{u}(l) = u(l) = u_{press} \end{cases} \tag{A.4}$$

defining now a control function v such that

$$v = 0 \; on \; \Gamma_D \tag{A.5}$$

and multiplying our initial equation by it

$$\int_0^l \left[\tilde{u} - c\frac{\mathrm{d}}{\mathrm{dx}}\left[\frac{d\tilde{u}}{dx}\right]\right] v \,\mathrm{dx} = \int_0^l uv \;\mathrm{dx} \tag{A.6}$$

separating the left integral and applying the by parts integration formula the obtained form is

$$\int_0^l uv \ \mathrm{dx} - cv(l)\frac{d\tilde{u}(l)}{dx} + cv(0)\frac{d\tilde{u}(0)}{dx} + \int_{\mathbf{0}}^{\boldsymbol{l}} c\frac{\mathrm{d}\tilde{u}}{\mathrm{dx}}\frac{\mathrm{d}v}{\mathrm{dx}}\mathrm{dx} = \int_0^l uv \ \mathrm{dx} \tag{A.7}$$

where if the boundary condition for all variables are applied the weak form obtained is

$$\int_0^l uv \ \mathrm{dx} + \int_{\mathbf{0}}^{\boldsymbol{l}} c\frac{\mathrm{d}\tilde{u}}{\mathrm{dx}}\frac{\mathrm{d}v}{\mathrm{dx}}\mathrm{dx} = \int_0^l uv \ \mathrm{dx} \tag{A.8}$$

Now, the three variables are defined in the following way

$$u \cong u^h(x) = \sum_{i=1}^{n} u_i N_i(x) \tag{A.9}$$

$$\tilde{u} \cong \tilde{u}^h(x) = \sum_{i=1}^{n} \tilde{u}_i N_i(x) \tag{A.10}$$

$$v = N_j(x) \tag{A.11}$$

and replacing it to the weak form obtained

$$\sum_{j=1}^{n}\sum_{i=1}^{n}\left[\int_0^l N_i(x)N_j(x) \ \mathrm{dx} + c\int_0^l N'_i(x)N'_j(x) \ \mathrm{dx}\right]\tilde{u}_i = \sum_{i=1}^{n}\left[\int_0^l N_i(x)N_j(x) \ \mathrm{dx}\right]u_i \tag{A.12}$$

defining the matrices as

$$M_{ij} = \int_0^l N_i(x)N_j(x) \ \mathrm{dx} \tag{A.13}$$

$$D_{ij} = c\int_0^l N'_i(x)N'_j(x) \ \mathrm{dx} \tag{A.14}$$

the regularization equation is

$$[\boldsymbol{M} + c\boldsymbol{D}]\tilde{\boldsymbol{u}} = \boldsymbol{M}\boldsymbol{u} \tag{A.15}$$

NEW MODEL

The new models include a term in the diffusion-reaction PDE so the diffusion parameter gets reduced with the increase of damage. All the formulation above is done explicitly for the new model with a bounded internal length reduction, but for the model with a vanishing internal length the results are the same only excluding the scalar parameter a.

The strong form of this model is

$$\tilde{u} - c\nabla[(1 - ad(\tilde{u}))\nabla\tilde{u}] = u \; in \; \Omega \tag{A.16}$$

$$\tilde{u}(x) = u(x) \qquad on \; \partial\Omega \tag{A.17}$$

applying this to our one dimension problem the strong form remains as

$$\tilde{u} - c\frac{\mathrm{d}}{\mathrm{dx}}\left[(1 - ad(\tilde{u}))\frac{d\tilde{u}}{dx}\right] = u \quad on \; x \in (0, l) \tag{A.18}$$

$$\begin{cases} \tilde{u}(0) = u(0) = 0 \\ \tilde{u}(l) = u(l) = u_{press} \end{cases} \tag{A.19}$$

defining now a control function v such that

$$v = 0 \; on \; \Gamma_D \tag{A.20}$$

and multiplying our initial equation by it

$$\int_0^l \left[\tilde{u} - c\frac{\mathrm{d}}{\mathrm{dx}}\left[(1 - ad(\tilde{u}))\frac{d\tilde{u}}{dx}\right]\right] v \,\mathrm{dx} = \int_0^l uv \;\mathrm{dx} \tag{A.21}$$

separating the left integral and applying the by parts integration formula the obtained form is

$$\int_0^l uv \;\mathrm{dx} - cv(l)\big(1 - ad(\tilde{u})\big)\frac{d\tilde{u}(l)}{dx} + cv(0)\big(1 - ad(\tilde{u})\big)\frac{d\tilde{u}(0)}{dx} + \int_0^l c(1 - ad(\tilde{u}))\frac{\mathrm{d}\tilde{u}}{\mathrm{dx}}\frac{\mathrm{d}v}{\mathrm{dx}}\mathrm{dx} = \int_0^l uv \;\mathrm{dx} \tag{A.22}$$

where if the boundary condition for all variables are applied the weak form obtained is

$$\int_0^l uv \;\mathrm{dx} + \int_0^l c(1 - ad(\tilde{u}))\frac{\mathrm{d}\tilde{u}}{\mathrm{dx}}\frac{\mathrm{d}v}{\mathrm{dx}}\mathrm{dx} = \int_0^l uv \;\mathrm{dx} \tag{A.23}$$

Now, the three variables are defined in the following way

$$u \cong u^h(x) = \sum_{i=1}^{n} u_i N_i(x) \tag{A.24}$$

$$\tilde{u} \cong \tilde{u}^h(x) = \sum_{i=1}^{n} \tilde{u}_i N_i(x) \tag{A.25}$$

$$v = N_j(x) \tag{A.26}$$

and replacing it to the weak form obtained

$$\sum_{j=1}^{n}\sum_{i=1}^{n}\left[\int_0^l N_i(x)N_j(x)\ \mathrm{dx} + c\int_0^l (1-ad)N'_i(x)N'_j(x)\ \mathrm{dx}\right]\tilde{u}_i = \sum_{i=1}^{n}\left[\int_0^l N_i(x)N_j(x)\ \mathrm{dx}\right]u_i \tag{A.27}$$

defining the matrices as

$$M_{ij} = \int_0^l N_i(x)N_j(x)\ \mathrm{dx} \tag{A.28}$$

$$D_{ij} = c\int_0^l (1-ad(\tilde{u}))N'_i(x)N'_j(x)\ \mathrm{dx} \tag{A.29}$$

the regularization equation is

$$[\boldsymbol{M} + c\boldsymbol{D}(\tilde{\boldsymbol{u}})]\tilde{\boldsymbol{u}} = \boldsymbol{M}\boldsymbol{u} \tag{A.30}$$

ANNEX B: LAGRANGE MULTIPLIERS

This annex focuses on the explanation on how the boundary conditions of the problem are treated using Lagrange multipliers.

In the problem presented and for all models there are two equations to be solved in each step

$$\boldsymbol{f_{int}}(u,\tilde{u}) + \boldsymbol{f_{reac_{equi}}} = \boldsymbol{f_{ext}} \tag{B.1}$$

$$[\boldsymbol{M} + c\boldsymbol{D}]\tilde{\boldsymbol{u}} + \boldsymbol{f_{reac_{regu}}} = \boldsymbol{M}\boldsymbol{u} \tag{B.2}$$

but in the new models the matrix $\boldsymbol{D}$ is nonlocal displacement dependant ($\boldsymbol{D}(\tilde{\boldsymbol{u}})$). For all models, there are two imposed boundary conditions

$$\tilde{u}(0) = u(0) = 0 \tag{B.3}$$

$$\tilde{u}(l) = u(l) = u_{press} \tag{B.4}$$

the Lagrange multipliers theory, see Belytschko et al. (2000), defines the matrix $\boldsymbol{A}$ and the vector $\boldsymbol{b}$ for this boundary conditions as

$$\boldsymbol{A} = \begin{pmatrix} 1 & 0 & \cdots & 0 \\ 0 & \cdots & 0 & 1 \end{pmatrix} \tag{B.5}$$

$$\boldsymbol{b} = \begin{pmatrix} 0 \\ u_{press} \end{pmatrix} \tag{B.6}$$

matrix $\boldsymbol{A}$ $(2\times n)$ defines the linear relations between the nodes for the boundary conditions and the vector $\boldsymbol{b}$ (2×1) is defined by the boundary conditions values. These matrices are the same for the equilibrium and regularization equation. So, the equation that determinate the boundary conditions are

$$\boldsymbol{A}\boldsymbol{u} = \boldsymbol{b} \tag{B.7}$$

$$\boldsymbol{A}\tilde{\boldsymbol{u}} = \boldsymbol{b} \tag{B.8}$$

allowing to compute at the reaction forces as

$$\boldsymbol{f_{reac_{equi}}} = \boldsymbol{A}\boldsymbol{\lambda}_{equi} \quad \text{(B.9)}$$

$$\boldsymbol{f_{reac_{regu}}} = \boldsymbol{A}\boldsymbol{\lambda}_{equi} \quad \text{(B.10)}$$

where $\boldsymbol{\lambda}$ are the called Lagrange multipliers. This method has some advantages

- General technique. Allowing multipoint restrictions.
- Reaction forcers appear clearly in both equations to be solved.
- The matrix $\boldsymbol{K}_{ii}$ is not modified, only the matrix $\boldsymbol{A}$ for the different boundary conditions.

and a main disadvantage

- The problem to solve has new variables to calculate at each step or iteration ($\boldsymbol{\lambda}_{equi}, \boldsymbol{\lambda}_{equi}$).

ANNEX C: APPROXIMATED VALUES WHEN SOLVING THE PROBLEM

In the new models the regularization equation is not linear anymore. Meaning that the matrix

$$\boldsymbol{K}_{\tilde{u}\tilde{u}} = \frac{\partial r_{regu}(\tilde{\boldsymbol{u}})}{\partial \tilde{u}} \tag{C.1}$$

should be recalculated in every step or iteration if the Newton method is wanted to be used exactly. Doing this calculation exactly the obtained result is

$${}^{k}\boldsymbol{K}_{\tilde{u}\tilde{u}}{}^{i} = \frac{\partial r_{regu}}{\partial \tilde{u}} = \boldsymbol{M} + c\boldsymbol{D}\left({}^{k}\tilde{\boldsymbol{u}}^{i}\right) + c\frac{d\boldsymbol{D}({}^{k}\tilde{\boldsymbol{u}}^{i})}{d\tilde{u}}\ {}^{k}\tilde{\boldsymbol{u}}^{i} \tag{C.2}$$

taking us to a calculation of a new matrix $\frac{d\boldsymbol{D}(\tilde{\boldsymbol{u}})}{d\tilde{u}}$ at each step, increasing the computational cost. The first approach to this problem was trying to reduce the computational cost approximating the real value for

$${}^{k}\boldsymbol{K}_{\tilde{u}\tilde{u}}{}^{i} = \frac{\partial r_{regu}}{\partial \tilde{u}} \approx \boldsymbol{M} + c\boldsymbol{D}\left({}^{k}\tilde{\boldsymbol{u}}^{i}\right) \tag{C.3}$$

with this approach, the calculation of the new matrix in each iteration is prevented, but the amount of iteration needed per step may increase. Implementing this in the code leaded to a non-convergence of the iterations. So, aiming for a compensation of errors ${}^{k}\boldsymbol{K}_{\tilde{u}\tilde{u}}{}^{i}$ has been approximated as

$${}^{k}\boldsymbol{K}_{\tilde{u}\tilde{u}}{}^{i} = \frac{\partial r_{regu}}{\partial \tilde{u}} \approx\ {}^{k}\boldsymbol{K}_{\tilde{u}\tilde{u}} = \boldsymbol{M} + c\boldsymbol{D}({}^{k}\tilde{\boldsymbol{u}}) \tag{C.4}$$

using the same diffusion matrix for all the iterations in each step. The results obtained were satisfactory, obtaining a nearly square converge with this method and reducing the overall computational cost.

BIBLIOGRAPHY

Bažant, Z. and Jirásek, M. (2002). Nonlocal integral formulations of plasticity and damage: Survey of progress. *Journal of Engineering Mechanincs 128* (11), 1119-1149. doi: 10.1061/(ASCE)0733-9399(2002)128:11(1119).

Bažant, Z. and Jirásek, M. (2001). *Inelastic Analysis of Structures*. Wiley.

Belytschko, T., W.K.Liu, and B. Moran (2000). *Nonlinear Finite Elements for Continua and Structures*. Wiley.

Bourdin, B., G. A. Francfort, and J.J. Marigo (2000). Numerical experiments in revisited brittle fracture. *Journal of the Mechanics and Physics of Solids 48* (4), 797-826. doi: 10.1016/S0022-5096(99)00028-9.

Casado-Antolín, M. (2016). A continuous-discontinuous model to introduce pressure in a crack. Degree's thesis, Universitat Politècnica de Catalunya, Departament d'Enginyeria Civil i Ambiental.

Crisfield, M. A. (1991). *Non-linear Finite Element Analysis of Solids and Structures*. Volume 1: Essentials. Wiley.

de Borst, R., J. Pamin, R. H. J. Perrlings, and L. J. Sluys (1995). On gradient-enhanced damage and plasticity models for failure in quasi-brittle and frictional materials. *Computational Mechanics 17* (1-2), 130-141. doi: 10.1007/BF00356485.

Hededal, O. and Krenk, S. (1995). FEMLAB. MATLAB Tollbox for the Finite Element Method Version 1.0. Aalborg University, Department of Building Technology and Structural Engineering. R/ Vol. R9450.

Mazars, J. and G. Pijaudier-Cabot (1996). From damage to fracture mechanics and conversely: A combined approach. *International Journal of Solids and Structures 33* (20-22), 3327-3342. doi: 10.1016/0020-7683(96)00015-7.

Peerlings, R. H. J., R. de Borst, W.A.M. Brekelmans, and M.G.D. Geers (1998). Gradient-enhanced damage modelling of concrete fracture. *Mechanics of Cohesive-frictional Materials 3* (4), 323-342. doi: 10.1002/(SICI)1099-1484(1998100)3:4<323::AID-CFM51>3.0.CO;2-Z.

R. de Borst, C. V. Verhoosel, Gradient damage vs phase-field approaches for fracture: Similariteis and differences, *Computer Methods in Applied Mechanics and Engineering* (2016), https://doi.org/10.1016/j.cma.2016.05.015.

Rabczuk, T. (2013). Computational Methods for Fracature in Brittle and Quasi-Brittle Solids: State-of-the-Art Review and Future Perspectives. *ISRN Applied Mathematics 2013*, 38 pages. doi: 10.1155/2013/849231.

Rodríguez-Ferran, A., I. Morata, and A. Huerta (2005). A new damage model base on non-local displacements. *International Journal for Numerical and Analytical Methods in Geomechanics 29* (5), 473-493. doi: 10.1002/nag.422.

Simo, J. C. and J.Oliver (1994). A new approach to the analysis and simulation of strain softening in solids. In *Fracutre and damage quasibrittle structures*, pp. 25-39.

Simeone, A., G. N. Wells, and L. J. Sluys (2003). From continuous to discontinuous failure in a gradient-enhanced continuum damage model. *Computer Methods in Applied Mechanics and Engineering 192* (41-42), 4581-4607. doi: 10.1016/S0045-7828(03)00428-6.

Tamayo-Mas, E. (2009). Continuous-discontinuous models of failure based on non-local displacements. Master's thesis, Universitat Politécninca de Catalunya.

Tamayo-Mas, E., Rodríguez-Ferran, A. (2011). Condiciones de controno en modelos gradiente con desplazamientos suavizados. Universitat Politècnica de Catalunya, Departament de Matemàtica Aplicada III.

Wells, G. N., L. J. Sluys, and R. de Borst (2002). Silmulating the propagation of displacement discontinuities in a regularized strain-softening medium. *International Journal for Numerical Methods in Engineering 53* (5), 1235-1256. doi: 10.1002/nme.375.